Self-assembly of Poly(ethylene oxide)-*b*-polystyrene-*b*-poly(acrylic acid) Triblock Copolymers in Solution

by

Qinghua Wu

A thesis submitted to McGill University
in partial fulfillment of the requirements for the degree of

Master of Science

Department of Chemistry
McGill University
Montréal, Québec
Canada
H3A 2K6

 August 2005

Your file Votre référence
ISBN: 978-0-494-24829-4
Our file Notre référence
ISBN: 978-0-494-24829-4

Abstract

The self-assembly behavior of poly(ethylene oxide)-*b*-polystyrene-*b*-poly(acrylic acid) (PEO-*b*-PS-*b*-PAA) triblock copolymers in solution is the focus of this thesis. The triblock copolymers were synthesized by atom transfer radical polymerization (ATRP). The compositions of the block copolymers were determined by ^{1}H NMR. The synthesized block copolymers have relatively low polydispersity indexes (PDI < 1.3) as proved by GPC. The influence of several factors on the ATRP of styrene or *t*-BA, such as temperature, catalyst and polymerization time, was also explored. The effects of several parameters on the self-assembly behavior of this triblock copolymer were investigated, including the nature and composition of the common solvent, PAA block length, pH, water content, and initial copolymer concentration. Multiple morphologies, such as spheres, vesicles, lamellae and rods have been prepared by varying the above parameters. In particular, vesicles with either PEO or PAA outside have been successfully prepared in dioxane/water. These vesicles may serve as carriers for potential encapsulation applications. The average size and corona chain composition of the triblock copolymer vesicles can be controlled by varying factors such as the PAA block length and pH. The polymer chains may have different arrangements in the vesicle wall, resulting in different corona chain compositions. The vesicles with PAA outside are stable in water, while the vesicles with PEO outside tend to flocculate. Nevertheless, the sediment can be redispersed under vigorous stirring.

Résumé

Le comportement d'auto-assemblage de copolymères triblocs de poly(oxyde d'éthylène)-*b*-polystyrène-*b*-poly(acide acrylique) (PEO-*b*-PS-*b*-PAA) consitute le sujet de recherche de cette thèse. Les copolymères triblocs ont été synthétisés par polymérisation radicalaire à transfert d'atome (ATRP). Les compositions des copolymères blocs ont été déterminées par ^{1}H RMN. Les copolymères blocs synthétisés ont une relativement petite faible polydispersité (PDI < 1.3) comme le montre la GPC. L'influence de plusieurs facteurs lors de la synthèse, tels que la température, la présence d'un catalyseur et le temps de polymérisation ont également été explorés. Les effets de plusieurs paramètres sur l'auto-assemblage de ce copolymère tribloc ont ensuite été étudiés : la nature et la composition du solvant, la longueur de bloc de PAA, le pH, la teneur en eau, et la concentration initiale en polymère. Des morphologies multiples, telles ques des sphères, des vésicules, des lamelles et des cylindres ont été préparées en faisant varier ces paramètres. En particulier, des vésicules avec le PEO ou le PAA à l'extérieur ont été préparées avec succès dans un mélange d'eau et de dioxane. Ces vésicules ont des applications potentielles d'encapsulation et de transport. La taille moyenne et la composition de la chaîne des vésicles peut être contrôlée en faisant varier la longueur des PAA et le pH. Les chaînes de polymères peuvent avoir différents arrangements dans les parois des vésicules, impliquant des compositions différentes des chaînes en couronne. Les vésicules avec les PAA à l'extérieur sont stables dans l'eau, tandis que celles avec les PEO à l'extérieur ont tendance à flocculer. Néanmoins, les sédiments peuvent être redispersés en agitant la solution vigoureusement.

Preface

This dissertation is comprised of five chapters. Chapter 1 provides a general introduction to the synthesis and self-assembly of amphiphilic block copolymers. In addition, brief introductions to the basics of polymer chemistry are included. The second chapter focuses on the synthesis and characterization of poly(ethylene oxide)-*b*-polystyrene-*b*-poly(acrylic acid) (PEO-*b*-PS-*b*-PAA) triblock copolymers. In chapter 3, the self-assembly behavior of the PEO-*b*-PS-*b*-PAA triblock copolymers in solution is described in detail. The effects of several parameters on the self-assembly behavior of this triblock copolymer are discussed, including the nature and composition of the common solvent, PAA block length, pH, water content, and initial copolymer concentration. Chapter 4 centers on the preparation and characterization of PEO-*b*-PS-*b*-PAA triblock copolymer vesicles. Vesicles with either PEO or PAA outside have been successfully prepared in dioxane/water. These vesicles may serve as carriers for potential encapsulation applications. The final chapter consists of the conclusions of the studies and suggestions for future work.

Contributions of Authors

Dr. Futian Liu synthesized the PS_{313}-*b*-PAA_{27} diblock copolymer by anionic polymerization. The PS_{313}-*b*-PAA_{27} diblock copolymer vesicles were prepared by the author and used in the zeta-potential measurements as described in Chapter 4. Other than the supervision, advice and direction of Dr. Adi Eisenberg, and the contribution mentioned above, all of the work presented in this dissertation was performed by the author.

Acknowledgements

I would like to express sincere thanks to my supervisor, Dr. Eisenberg, for his support of my research, and for his invaluable advice during the preparation of this thesis.

My heartfelt appreciation to Futian, Owen, and Tony, for passing on their knowledge and knowhows on polymer synthesis and characterization to me. Many thanks to Nicolas for volunteering in the preparation of the résumé since my French is at the beginner's level. Thanks also go to the other group members, past (Amira, Carl, Patrick, Shing and Xiaoya) and present (Alex, Jun, Renata, and Xingfu), for providing a pleasant environment in which to learn and mature.

I would also like to extend earnest thanks to other fellow graduate students, Faisal, Hua, Iran, Loiza, Paul, Petr, and Yingdong, for sharing their knowledge of different techniques such as IR, NMR, carbon coating of copper grids and electrophoresis.

A sincere thank you to George for his help in restoring our glassware. I am also grateful to Fred and Rick for their help with any instrument that breaks down. I would also like to thank Jeannie, Kelly and Dr. Vali for their training and advice on TEM.

A special thank you to other staff members, Carol, Chantal, Fay, Renée, and Sandra, for their assistance in everything ranging from visa applications to room reservations for group meetings.

Finally, I am forever in debt to my family and friends, wherever they are, particularly Mum and Dad, and Frank, my sweetheart. And I cannot leave out my cat, Mimi. Everyday, she meows at my door for hours in the morning between 6:00 to 8:00 until I wake up...☺

Table of Contents

List of Tables

List of Figures

Chapter 1

General Introduction

1.0 Introduction

Amphiphilic block copolymers in selective solvents, like natural lipids, can self-assemble into aggregates with different morphologies, including spheres, rods and vesicles. These self-assembled structures have potential for various applications such as drug delivery and cosmetics. Recently, block copolymer vesicles have attracted considerable interest. For instance, vesicles with asymmetric membrane structures have been prepared from ABC-type triblock copolymers with hydrophilic blocks A and C and a hydrophobic middle block B.[1-2]

This thesis focuses on the synthesis and the self-assembly of a new type of triblock copolymer, poly (ethylene oxide)-*b*-polystyrene-*b*-poly(acrylic acid) in solution as well as vesicle preparation from this triblock copolymer. Several factors that affect the synthesis and the self-assembly were investigated. In addition, vesicles with different sizes and corona chain compositions were prepared by varying factors such as the block length of the poly (acrylic acid) and the pH.

This chapter is divided into four sections: the first section provides some necessary background materials on polymer chemistry; the second describes the most widely used methods for block copolymer synthesis and the polymer characterization techniques used in this thesis; the third discusses the self-assembly of block copolymers in bulk and in solution; finally, a summary of the overall scope of the thesis is presented.

1.1 Some Basic Definitions of Polymers

Some fundamental concepts need to be introduced before discussing the synthesis and the self-assembly of block copolymers.

1.1.1 Polymers

The term polymer is a composite of the Greek words "poly" and "meros", meaning "many parts".[3] Polymers, or macromolecules, are large molecules made of many smaller repeating structural units called monomers that are covalently bonded together. The process by which monomers link together to form a molecule of a relatively high molecular mass is known as polymerization. If only one type of monomer is used during polymerization, a homopolymer is generated. When two or more species of monomers are involved in polymerization, a copolymer is created. According to the way that different structural units are distributed in the polymer chains, copolymers can be further subdivided into statistical copolymers, alternating copolymers, block copolymers and graft copolymers (Fig. 1.1).[4]

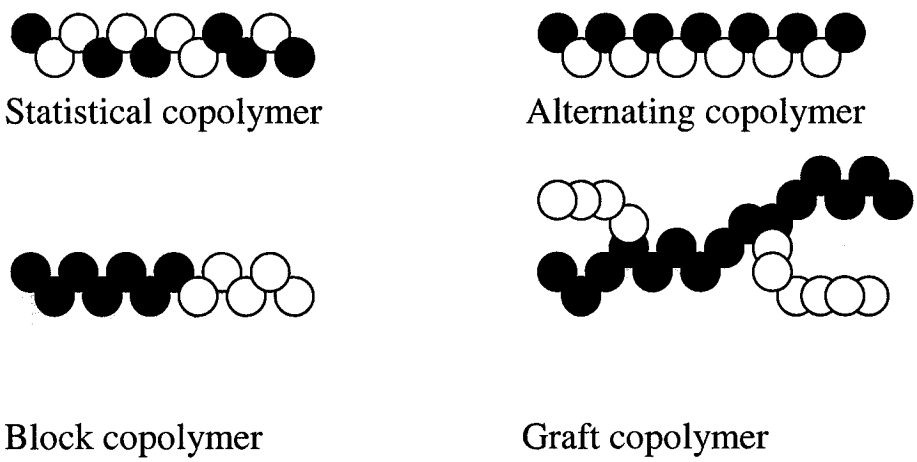

Fig. 1.1 Schematic representation of statistical, alternating, block and graft copolymers.

1.1.2 Average Molecular Weights and Molecular Weight Distributions

One distinguishing feature of synthetic polymers is that they usually have a distribution of molecular weights due to the random events affecting the formation of chains during polymerization. The distribution depends on the polymerization method. Consequently, polymers are best characterized by average molecular weights and the associated molecular weight distributions. There are many ways to determine an average molecular weight. The type of property being studied will determine the techniques that need to be used and the resulting type of average molecular weight. For example, strength properties may be influenced more by high molecular weight molecules than by low molecular weight molecules, therefore sedimentation equilibrium method can be employed to obtain the z-average molecular weight that emphasizes the high molecular weight portion.[5]

Similar to colligative properties of dilute solutions, the number average molecular weight (M_n) is only sensitive to the number of polymer molecules present, defined as the total weight of polymer divided by the number of polymer molecules as shown in equation (1-1),[6] where N_i is the number of polymer molecules with the molecular weight M_i. The term $N_i/\Sigma N_i$ is the number fraction of polymers with molecular weight Mi. This average molecular weight follows the conventional definition for the mean value of any statistical quantity.

$$M_n = \Sigma N_i M_i / \Sigma N_i \qquad (1\text{-}1)$$

By replacing N_i in the number average molecular weight formula with N_iM_i, the result is the weight average molecular weight (M_w), depending not only on the number of

polymer molecules but also on the size or weight of each polymer molecule.[6] The term $N_iM_i/\Sigma N_iM_i$ is the weight fraction of polymers with molecular weight Mi.

$$M_w = \Sigma N_i M_i^2 / \Sigma N_i M_i \qquad (1\text{-}2)$$

The meanings of the words are thus apparent—the number average molecular weight is the average molecular weight weighted according to number fractions and the weight average molecular weight is the average molecular weight weighted according to weight fractions.

If N_i in (1-1) is replaced by $N_iM_i^k$, an average molecular weight denoted as M_k can be obtained:

$$M_k = \Sigma N_i M_i^{k+1} / \Sigma N_i M_i^k \qquad (1\text{-}3)$$

Thus $M_0 = \Sigma N_i M_i / \Sigma N_i = M_n$, and $M_1 = \Sigma N_i M_i^2 / \Sigma N_i M_i = M_w$. Several other higher average forms appear in experiments.[6] For instance, $M_2 = M_z$ can be determined by sedimentation equilibrium technique and used in describing mechanical properties.[7]

One average molecular weight which does not fit into the mold of M_k is the viscosity average molecular weight M_v, defined as the following, where α is a constant that depends on the polymer/solvent pair used in the viscosity experiments:[8]

$$M_v = [\Sigma N_i M_i^{\alpha+1} / \Sigma N_i M_i]^{1/\alpha} \qquad (1\text{-}4)$$

For monodisperse polymers, all the molecular weight averages are the same; however, for polydisperse polymers, all the average molecular weights will be different and will rank in the following order:[6]

$$M_n < M_v < M_w < M_z < M_{z+1} < M_{k,\,k\geq 4} < M_{k+i,\,k\geq 4\,,\,i\geq 1} \qquad (1\text{-}5)$$

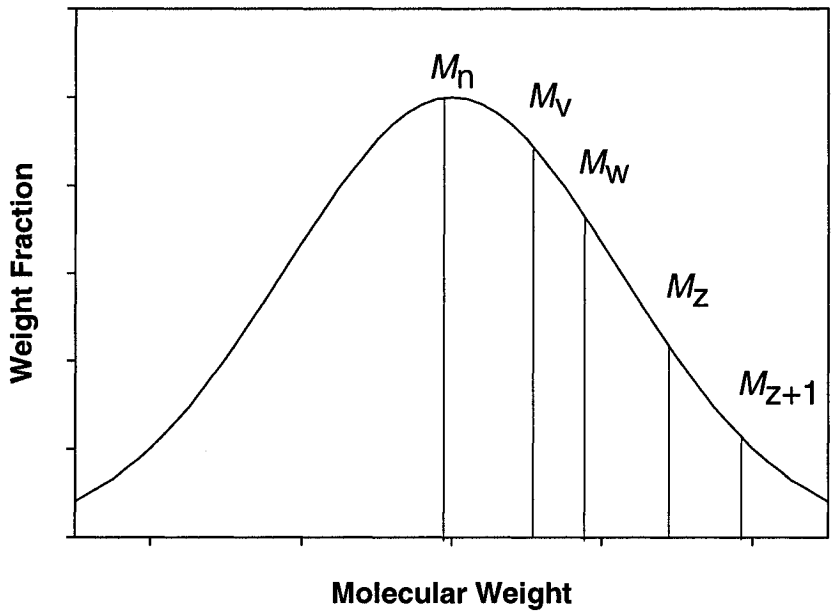

Fig. 1.2 Schematic of a typical distribution of molecular weights for a synthetic polymer.

The typical molecular weight distribution of a synthetic polymer may look like that shown in Fig. 1.2, resembling a Gaussian distribution curve. The various average molecular weights are indicated in their expected rank. The breadth of the distribution can be characterized by the polydispersity index (M_w/M_n).[6] The polydispersity index must be greater than or equal to one. When it is equal to one, the distribution is monodisperse. For a synthetic polymer, the polydispersity index is generally greater than one and the amount by which it is greater than one is a measure of the polydispersity of that polymer.

1.2 Synthesis and Characterization of Block Copolymers

Block copolymers have attracted considerable attention because of their technical importance for various applications such as thermoplastic elastomers, pressure sensitive

adhesives, and impact modifiers. The synthesis of block copolymers provides an additional method of creating new materials besides the synthesis of new monomers for polymerization, and physical blending of polymers. Most of the block copolymers have been prepared by ionic polymerization, especially anionic polymerization. In the past decade, controlled radical polymerization has been developed, representing a useful alternative synthetic approach. Below are some features of ionic polymerization and two typical controlled radical polymerization methods.

1.2.1 Ionic Polymerization

Ionic polymerization has been successful for decades in the synthesis of block copolymers with well-defined structures. Under appropriate experimental conditions, due to the absence of termination and chain transfer reactions, the ionic sites remain active after the complete consumption of one monomer, giving the possibility of block copolymer formation by the sequential ionic polymerization of different monomers.

Ionic polymerization is a chain polymerization in which the kinetic-chain carriers are ions or ion pairs.[9] This type of polymerization is specific for monomers that can form stable carbenium ions or carbanions. Consequently, the species of monomers are usually limited to those with strong electron-donating or electron-withdrawing groups. The most common cationically polymerizable monomers are isobutylene, vinyl ethers, styrene and its derivatives with electron donating groups, furan, and some other heterocyclic monomers. And the most common anionically polymerizable monomers include acrylonitrile, vinyl chloride, styrene, and methyl methacrylate.

The initiation of cationic polymerization could be accomplished by classical protonic acids, Lewis acids or carbenium ion salts.[9] By contrast, the initiators for anionic

polymerization are usually organometallic compounds including *n*-butyl lithium, diphenyl-methyl potassium, and Grignard reagents.[9] In either case, the initiation step of polymerization is rapid with a reaction rate much larger than that of the propagation step so that all active sites start polymerizing the monomer almost at the same time. As a result, polymers with narrow molecular weight distributions could be prepared.

The chain propagation step proceeds rapidly at low temperature, depending on many factors, such as the solvent, the initiator, the counter-ion, the temperature and the inhibitors.[9] Ionic-initiated polymerizations are complex processes whose mechanisms are often difficult to clarify. For example, even small quantities of water will significantly affect the polymerization rate in cationic polymerization.

The termination step is not desired but could happen in a cationic polymerization due to a unimolecular rearrangement of the ion pair or a transfer reaction with the monomer which can be suppressed by using an appropriate counter-ion and a carefully selected Lewis base.[10] Despite the fact that there is no formal termination step for anionic polymerization, this type of polymerization is sensitive to traces of impurities such as water, alcohol, carbon dioxide, and oxygen since they can neutralize the carbanions. Therefore, rigorous experimental procedures are needed to eliminate impurities for anionic polymerization.[11]

1.2.2 Controlled Radical Polymerization

Free radical polymerization is widely used for the industrial preparation of polymers such as LDPE and PVC. A wide range of monomers can be polymerized by free radical polymerization under less rigorous experimental conditions compared with

ionic polymerization. However, for mixtures of monomers, only polydisperse copolymers with statistical molecular structures can be prepared due to the presence of automatic termination and chain transfer reactions. Recently, different controlled radical polymerization methods have been developed to eliminate or suppress the undesired termination and chain transfer reactions. There are two main approaches for bock copolymer synthesis: stable free radical polymerization[12] and atom transfer radical polymerization.[13]

1.2.2.1 Stable Free Radical Polymerization

Stable free radical polymerization (SFRP) is a controlled radical polymerization technique involving in the use of stable free radical nitroxides, *e.g.*, 2,2,6,6-tetramethylpiperidinoxy (TEMPO).[12] The mechanism of SFRP is shown in Fig. 1.3.

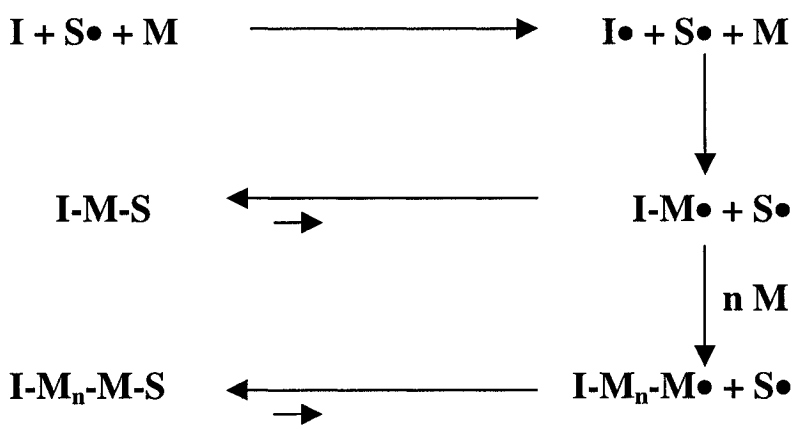

Fig. 1.3 Schematic of SFRP mechanism.[12]

The stable free radical nitroxides (**S•**) do not initiate polymerization. Instead, the polymerization is initiated with regular initiators (**I**) such as azobisisobutyronitrile (AIBN) and benzoyl peroxide. Above the decomposition temperature, the initiator will

undergo homolytic cleavage to yield two active free radicals (**I•**), which will then react with the monomers (**M**) to form macroradicals (**I-M•**). The majority of the macroradicals will interact with the stable nitroxide radicals to form dormant chains (**I-M-S**) that can not react with the monomers. However, the dormant chains can undergo reversible homolytic cleavage to regenerate the active radical site and then grow by the addition of new monomer units. In this way, the termination of chains are suppressed since the concentration of active free radicals remains low. In addition, the rapid exchange between dormant and active species enables the synthesis of block polymers with narrow molecular weight distributions.

1.2.2.2 Atom Transfer Radical Polymerization

Atom transfer radical polymerization (ATRP) mediated by a variety of transition metal complexes is one of the most widely used controlled radical polymerization techniques. The normal ATRP mechanism[13] is presented in Fig. 1.4.

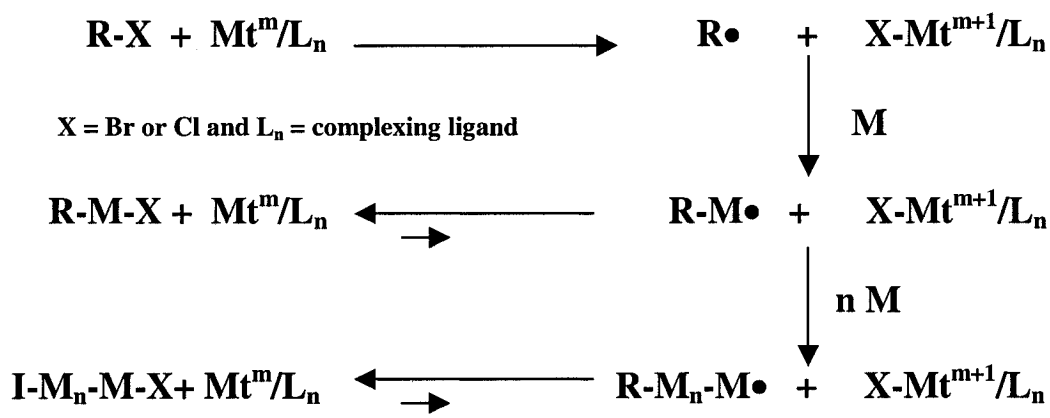

Fig. 1.4 Schematic of normal ATRP mechanism.[13]

The polymerization is initiated by a halogen transfer between a dormant species (**R-X**) and a transition metal complex ($\mathbf{Mt^m/L_n}$), resulting in the formation of active radicals (**R•**) and the metal complex in the higher oxidation state ($\mathbf{X\text{-}Mt^{m+1}/L_n}$), the deactivator.[16] The active radicals propagate by the addition of monomers to form macroradicals (**R-M•**) which can reversibly react with oxidized metal complexes to reform the dormant species (**R-M-X**) and the transition metal complex in the lower oxidation state, the activator. The propagation step consists of a series of monomer addition to the active radicals through halogen exchange. This is another way of keeping the concentration of active radicals low, suppressing termination reactions. Furthermore, the rapid halogen exchange facilitates the synthesis of block copolymers with relatively low polydispersities ($M_w/M_n < 1.5$).

1.2.3 Polymer Characterization

After synthesis, the polymers need to be characterized by a combination of analytical techniques to obtain their compositions, average molecular weights, polydispersities and other desired properties. A variety of analytical techniques are now available for the characterization of polymers. In this thesis, three techniques were employed to obtain the block copolymer composition, molecular weights and polydispersities.

1.2.3.1 Infrared Spectroscopy

Infrared spectroscopy (IR) is useful in the determination of different infrared active functional groups present along the polymer chain.[14] Each functional group has a unique vibrational frequency that can be used to determine what functional groups are in

a sample. When the effects of all the different functional groups are taken together, the result is a unique molecular "fingerprint" that can be used to confirm the identity of a sample. However, IR is not a practical tool for identifying the entire structure of the sample. In this thesis, IR was preferably used to confirm the hydrolysis of *t*-butyl acrylate groups.

1.2.3.2 Nuclear Magnetic Resonance

Quantitative information with respect to copolymer composition can be obtained by nuclear magnetic resonance (NMR). The absorption peak or chemical shift of a nucleus is related to its chemical environment. Thus, the structure of a sample can be determined by comparing the chemical shifts on the spectrum to known values of chemical shifts.[15] In this thesis, ^{1}H NMR was employed to calculate the relative numbers of styrene and *t*-butyl acrylate repeating units in the block copolymers.

1.2.3.3 Gel Permeation Chromatography

Gel permeation chromatography (GPC), also known as size exclusion chromatography (SEC), is a relative method that yields not only the average molecular weights but also the molecular weight distribution of a polymer sample. In comparison, the absolute methods, such as osmomotry and light scattering, only give a single average molecular weight.

A GPC instrument consists of five main components: injector, pump, column set, detector and automatic data processing equipment.[16] The polymer sample solution is introduced into the flowing system by the injector and then delivered through the

columns and system by the pump. The detector records the separation and the results are automatically calculated by the data processing system.

Polymer molecules with different sizes are separated by the columns according to their effective sizes in solution.[16] To prepare a sample for GPC analysis, the polymer sample is first dissolved in an appropriate solvent. The sample solution is then injected into a continually flowing stream of solvent that flows through a large number of highly porous, rigid particles tightly packed together in a column. The large molecules are not able to enter the small pores and thus pass quickly through the column, while the small molecules can diffuse into more small pores and thus stay longer in the column before being eluted. The width of the peak reflects the distribution of the sizes of molecules for a given polymer sample. The broader the peak, the broader the molecular weight distribution.

A calibration curve is needed in order to assign a molecular weight to each retention time for a polymer sample. There are several ways to do a calibration, but the most convenient is the conventional narrow standard calibration technique based on a set of well-characterized polymer standards with narrow molecular weight distributions.[16] However, the molecular weight averages obtained by this calibration method are relative to the calibrant. For example, if the column set is calibrated with polystyrene standards and the sample is poly(ethylene oxide), the molecular weights obtained after integration would be based on polystyrene, and be incorrect for poly(ethylene oxide).

In this thesis, the conventional narrow standard calibration technique based on polystyrene standards was used, so the molecular weights obtained for the block copolymers are based on polystyrene and appear incorrect in most cases. Consequently,

NMR was used to obtain the compositions and molecular weights of block copolymers instead. Nevertheless, GPC is invaluable in determining the molecular weight distributions of the block copolymers.

1.3 Self-assembly of Block Copolymers

Block copolymers have been used primarily as thermoplastic elastomers and compatibilizers for polymer blends. The phase behavior of block copolymers in bulk has been studied extensively since the 1960s. In the past decade, the self-assembly behavior of amphiphilic block copolymers in solution has been a subject of extensive research, due to the great potential to employ these self-assembled structures in drug delivery and many other applications.

Block copolymers are composed of chemically distinct blocks covalently linked together. The different blocks are usually immiscible and will undergo microphase separation in bulk or in solution. Various morphologies including lamellae, spheres and cylinders have been prepared both in bulk and in solution. The formation of different morphologies is controlled by many factors such as the copolymer composition and temperature. In the following sections, the main factors that control the self-assembly of block copolymers in bulk and in solution will be discussed.

1.3.1 Self-assembly in Bulk

A block copolymer can self-assemble in bulk to form nanoscale structures with a domain spacing typically in the range 10–200 nm. The characteristic dimensions of the morphologies depend on the molecular architecture of the copolymer, the molecular

weight of the copolymer, the volume fraction of the components, and the strength of interactions between the different blocks, represented by the Flory–Huggins interaction parameter (χ) between the different blocks.[17]

For the simplest AB diblock copolymers, the morphologies depend on three parameters: the molecular weight of the copolymer, the volume fraction of A block and the interactions between A and B blocks, indicated by χ_{AB}. If the incompatibility of the two blocks are sufficient, the copolymer will undergo microphase separation in bulk to form ordered morphologies. Four stable morphologies have been found: lamellar, cylindrical, spherical, and gyroid structures, as confirmed by both theory[18] and experiment.[19]

For ABC triblock copolymers, the number of molecular parameters is significantly increased: there are two independent composition variables (volume fractions f_A and f_B), three χ parameters (χ_{AB}, χ_{AC} and χ_{BC}) and three possible block sequences (ABC, BAC and ACB), leading to more possible combinations of these molecular parameters and new complex morphologies. A variety of morphologies have been found for linear ABC triblock copolymers, including lamellae, cylinders, spheres, gyroids and mixed microstructures[20], as well as some complex structures such as networks.[21] For multiblock copolymers, the combinations of molecular parameters are drastically expanded, giving the possibility of forming still more complex structures.

1.3.2 Self-assembly in Solution

Amphiphilic block copolymers, like small surfactants, can self-assemble in solution to yield a spectrum of morphologies such as spheres, rods, and vesicles.

However, asymmetric amphiphilic block copolymers with long hydrophobic blocks are usually not soluble in water, so a common solvent such as THF is needed to first dissolve the copolymer; self-assembly is then induced by the slow addition of water, which is a precipitant for the hydrophobic segment. In the following sections, the basic concepts related to the self-assembly are first introduced before discussing the morphologies of the aggregates, the factors controlling the formation of different morphologies and aggregate characterization techniques.

1.3.2.1 Critical Water Content and Critical Micelle Concentration

Aggregates can be prepared by the slow addition of water into a homogeneous amphiphilic block copolymer solution. When the added water reaches some critical value, a microphase separation occurs and aggregates start to form. This critical amount of added water is called critical water content (CWC).

The CWC of a homogeneous amphiphilic block copolymer solution essentially depends on three factors: the molecular weight of the hydrophobic block, the common solvent, and the initial copolymer concentration.[22] It has been found that, for the same solvent and initial copolymer concentration, the CWC decreases as the molecular weight of hydrophobic polystyrene block increases. The CWC is also affected by the nature of the common solvent that is used to dissolve the amphiphilic block copolymer. For PS-*b*-PAA diblock copolymers, the CWC is usually around 5.0% w/w in DMF, 10% w/w in dioxane and 20% w/w in THF.[23] In addition, CWC is related to the initial copolymer concentration as shown in equation (1-6),[22] where A and B are constants for a certain copolymer. As indicated by the equation, the higher the initial copolymer concentration, the lower the CWC.

$$CWC = -A \log C_0 + B \qquad (1\text{-}6)$$

The critical micelle concentration (CMC) is another important parameter. Only if the concentration of the copolymer is above CMC, could aggregates start to form. The CMC depends on various factors including the composition of the copolymer as well as the solvent. The CMC is closely related to the CWC. At the CWC, the aggregates start to form and thus the concentration of the copolymer at CWC represents the CMC.

1.3.2.2 Morphologies of Amphiphilic Block Copolymers in Solution

In selective solvents, amphiphilic block copolymers can self-assemble into aggregates. In a polar solvent, regular micelles with a hydrophobic core and a hydrophilic corona are formed, while in a solvent of low polarity, reverse micelles with the opposite structure are made. Depending on the relative length of the corona block, micelles can be further divided into two categories: star-like micelles with much longer corona chains, and crew-cut aggregates that have much shorter corona chains compared with the size of the core chains.[24]

In 1995, Zhang and Eisenberg[25] first reported the systematic preparation of various 'crew-cut' aggregate morphologies from asymmetric PS-*b*-PAA diblock copolymers in solution. Some of the observed morphologies are presented in Fig. 1.5[26], including spheres, rods, vesicles, small lamellae and sheets of lamellae, as well as some complex structures, such as bicontinuous rods, hexagonally packed hollow hoop structures (HHH), and large compound micelles (LCM).

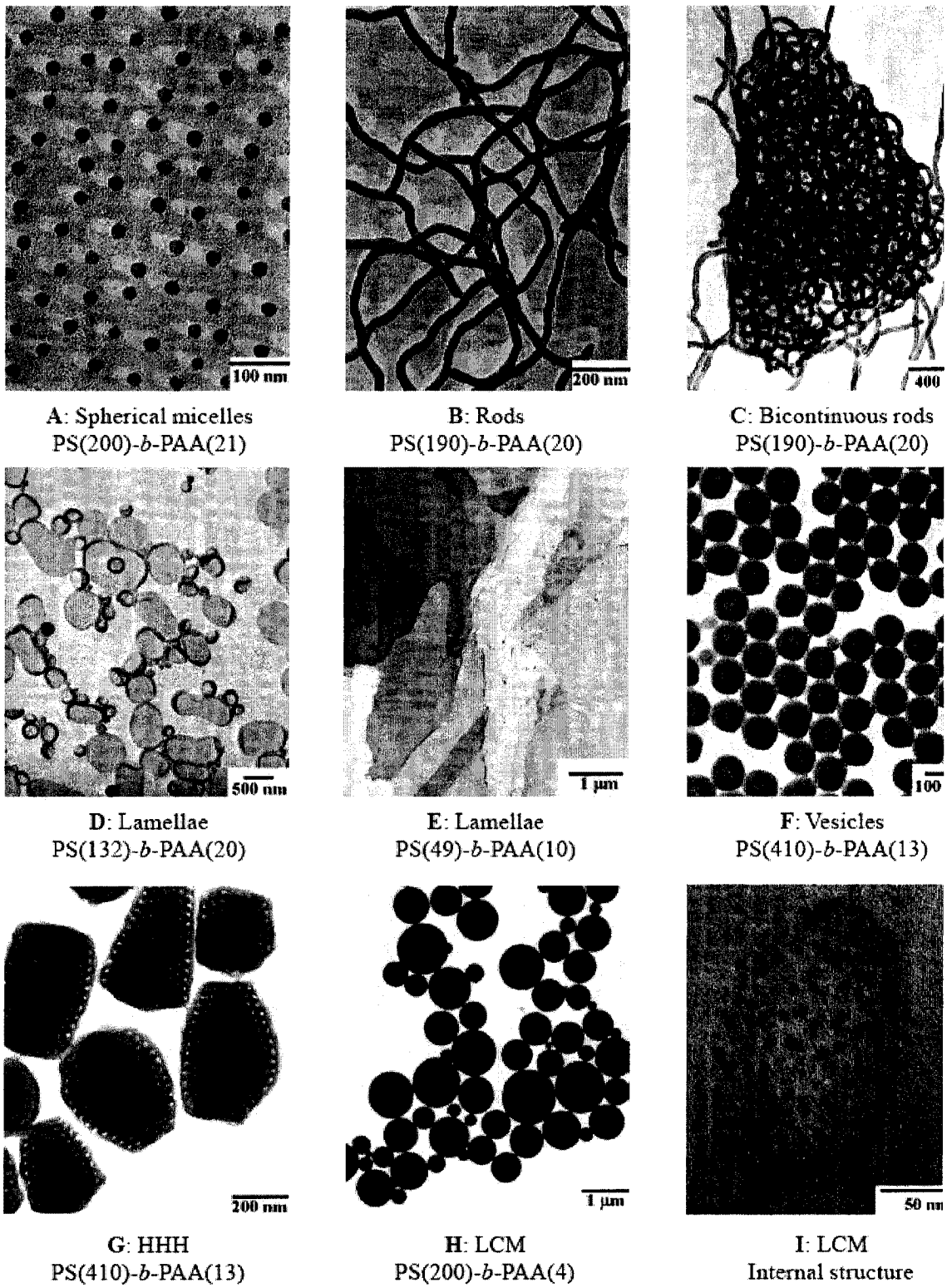

A: Spherical micelles
PS(200)-*b*-PAA(21)

B: Rods
PS(190)-*b*-PAA(20)

C: Bicontinuous rods
PS(190)-*b*-PAA(20)

D: Lamellae
PS(132)-*b*-PAA(20)

E: Lamellae
PS(49)-*b*-PAA(10)

F: Vesicles
PS(410)-*b*-PAA(13)

G: HHH
PS(410)-*b*-PAA(13)

H: LCM
PS(200)-*b*-PAA(4)

I: LCM
Internal structure

Fig. 1.5 TEM images of different morphologies prepared from PS-*b*-PAA diblock copolymers.[26]

1.3.2.3 Factors Controlling the Formation of Different Morphologies

A number of factors have been found effective in controlling the morphologies of diblock copolymers in solution. The control mechanisms of several factors related to the study described in Chapter 3 are explained by considering the force balance of three factors: the corona-chain repulsion, the core-chain stretching and the interfacial tension between the core and the outside solution.[25]

1.3.2.3.1 Common Solvent

The nature of the common solvent has a significant effect on the aggregate morphology. For PS-*b*-PAA diblock copolymers, spheres are usually found in DMF, while in dioxane or THF, bigger aggregates such as vesicles and LCMs can be prepared.[27-28] The formation of various morphologies is controlled by the polymer-solvent interactions. The interactions between the PS core and the solvent can be estimated by comparing the solubility parameter of homo-PS with those of the solvents, while the dielectric constants of the solvents can be used to estimate the degree of corona chain repulsion, as suggested by Yu and Eisenberg.[28] The solubility parameter of dioxane or THF is closer to that of homo-PS than that of DMF, so the solvent content in the PS core is higher in dioxane or THF, resulting in a higher degree of core chain stretching. To minimize the entropy penalty, spherical micelles would change their morphology to rods or to vesicles when the solvent is changed from DMF to dioxane or THF. In addition, the dielectric constant of dioxane or THF is lower than that of DMF, and thus a lower degree of ionization of acrylic acid groups is expected in dioxane or THF, leading to a lower degree of corona chain repulsion that also favors the formation of bigger aggregates since more chains are allowed to assemble in the same aggregate.

1.3.2.3.2 Water Content

The water content may affect both the morphology and the size of the aggregates. For PS-*b*-PAA diblock copolymers, spheres usually form first during the water addition process; as the water content increases, the morphologies may change progressively from spheres, to rods and to vesicles.[29-30] With increasing water content, the interfacial tension between the hydrophobic polystyrene chains and the outside solution increases, favoring the formation of bigger aggregates to minimize the total interfacial area. As the size of the aggregates becomes bigger, the core-chain stretching also becomes bigger. Due to the increasing entropy penalty, the core size cannot increase indefinitely. Under certain conditions, the aggregates would change their morphologies from spheres, to rods, and to vesicles to decrease the degree of core-chain stretching.[29-30] As more water is added, more acrylic acid groups are ionized, resulting in a higher degree of corona chain repulsion that facilitates the formation of smaller aggregates. For crew-cut aggregates, the corona chains are very short, so the core-chaining stretching is more important, resulting in the morphological changes as described above.

1.3.2.3.3 Hydrophilic Block Length

The hydrophilic block length may also affect the aggregate morphology. For PS-b-PAA diblock copolymers, as the content of PAA decreases, the aggregate morphology may change from spheres, to rods, to vesicles, to lamellae and to LCMs.[25,31] The decrease of the PAA block length results in the decrease of the corona chain repulsion. Consequently, more chains are allowed to assemble in the same aggregate, leading to a

higher degree of core-chain stretching. To compensate the entropy penalty, the morphological changes as described above will occur with .decreasing PAA content.

1.3.2.3.4 pH

pH is also a morphogenic factor since PAA is pH responsive.[32-33] The corona chain repulsion is responsible for the formation of various aggregate morphologies at different pH. At low pH, the degree of ionization of acrylic acid is low, corresponding to a low degree of corona chain repulsion that contributes to the formation of bigger aggregates. With increasing pH, the degree of ionization of acrylic acid also increases, resulting in increasing corona chain repulsion that facilitates the formation of smaller aggregates. However, the size of the aggregates cannot decrease indefinitely due to the increasing interfacial energy. At certain points, the aggregates would change their morphologies from vesicles to rods, and to spheres.

1.3.2.3.5 Initial Copolymer Concentration

The initial copolymer concentration can also be used to control the aggregate morphology. With increasing initial copolymer concentration, the aggregate morphology may change progressively from spheres, to rods, and to vesicles.[30] As the initial copolymer concentration increases, the core size also increases to minimize the interfacial area, leading to a higher degree of core-chain stretching. As discussed before, the increase of the aggregate size is limited by the entropy penalty. Instead, at certain conditions, the aggregates would change their morphologies as described above.

1.3.2.4 Aggregate Characterization

After preparation, the aggregates need to be characterized in terms of morphology, size and size distribution, corona chain composition *etc.* Many techniques are available for characterizing aggregates. For instance, the sizes of the aggregates can be obtained by light scattering, neutron scattering and many imaging techniques, *e.g.*, transmission electron microscopy (TEM). In this thesis, three characterization techniques were used: turbidity measurements using a UV-Vis instrument, TEM and electrophoresis.

1.3.2.4.1 Turbidity Measurement

Turbidity measurement is useful in measuring CWC as well as monitoring the morphological transitions by plotting turbidity or absorbance against water content. An example of a turbidity diagram is given in Fig. 1.6.[34] The turbidity as a function of water content shows three sharp jumps associated with three morphological transitions from single chains to spheres, from spheres to rods, and from rods to vesicles.[29,34] It should be noted that the morphological transitions are usually not as sharp jumps as those shown in Fig. 1.6.

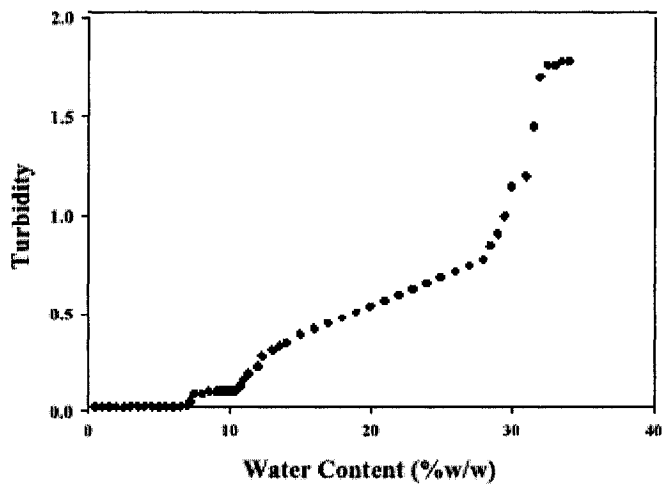

Fig. 1.6 Turbidity diagram of 1.0% (w/w) PS_{310}-*b*-PAA_{52} in dioxane.[34]

1.3.2.4.2 Transmission Electron Microscopy

The transmission electron microscope operates on the same basic principles as the light microscope, except that electrons are used instead of light.[34] The resolution of a light microscope is limited by the wavelength of the light source, while TEM uses electrons for illumination. The small wavelength of electrons makes it possible to get a resolution a thousand times better than that of a light microscope. The high magnifications which are accessible have made TEM invaluable in various fields including biology and materials science.

The imaging process is as follows.[34] First, an electron gun at the top of the microscope emits the electrons that travel through vacuum in the column of the microscope, continually focused by a series of electromagnetic lenses into a very thin beam. The thin beam then travels through the specimen. Depending on the density of the materials present, some of the electrons are scattered and disappear from the beam. At the bottom of the microscope the unscattered electrons hit a fluorescent screen, generating an image of the specimen. The image can be studied directly or photographed with a camera.

1.3.2.4.3 Electrophoresis

Electrophoresis is the movement of charged colloidal particles under the influence of an electric field.[35] The colloidal particles are surrounded by the liquid. An imaginary surface called the shear plane separates the thin layer of liquid bound to the particle surface from the rest of liquid. The electric potential at the shear plane is the zeta potential (ζ) which is proportional to the electrical mobility (m) of the particles, as shown in equation (1-8). This equation is valid for spherical particles. In this equation, ε is the

permittivity of the suspending medium and η its viscosity. $f(\kappa a)$ is a correction factor whose value is a function of the electric double layer thickness. The particle radius is a and $f(\kappa a)$ can be estimated from the calculations by O'Brien and White.[36]

$$\zeta = 3 \text{ m } \eta / 2 \varepsilon f(Ka) \qquad (1\text{-}8)$$

Electrophoresis is widely used in the separation of charged particles such as proteins and polysaccharides. In this thesis, electrophoresis is employed to determine the zeta-potential values of different copolymer vesicles as a function of pH. By comparing the zeta-potential curves of the triblock copolymer vesicles with those of PS-*b*-PEO and PS-*b*-PAA vesicles, one can see qualitatively the external corona chain compositions of the triblock copolymer vesicles.

1.4 Objectives of this Thesis

The objectives of the research presented in this thesis were to synthesize a new type of triblock copolymer, to investigate factors that affect the self-assembly behavior of this triblock copolymer, and to prepare vesicles with asymmetric membranes that may serve as carriers for potential encapsulation applications. In this introduction, a general overview as well as the necessary background materials is provided for an understanding of the studies presented in the following chapters.

Chapter 2 focuses on the synthesis of PEO-*b*-PS-*b*-PAA triblock copolymers using a controlled polymerization technique, atom transfer radical polymerization (ATRP). Controlled radical polymerization (CRP) techniques can generate well-defined polymer structures by a control of the statistical process of radical polymerization without

introducing the strict reaction conditions of anionic polymerization. In the past decade, several CRP techniques have been developed, and in this chapter the choice of ATRP as the polymerization technique used in the synthesis of the materials described in this thesis is elucidated. ATRP is a technique that depends on many variables and the influence of some of these variables such as temperature, solvent and polymerization time is discussed.

In chapter 3, the self-assembly of this triblock copolymer into different morphologies is described. The effects of several factors on the aggregate size and morphology are discussed, including the nature and compositions of the common solvent, PAA block length, pH, water content and initial copolymer concentration. Multiple morphologies, including spheres, vesicles, lamellae and rods, can be prepared by varying the above factors.

Chapter 4 centers on the preparation and characterization of triblock copolymer vesicles. Vesicles with asymmetric membrane structures (either PEO or PAA outside) may serve as vehicles for potential encapsulation applications. The average size and corona chain composition of the triblock copolymer vesicles can be controlled by varying factors such as the PAA block length and pH. The possible arrangements of the polymer chains in the vesicle wall and the stability of the vesicles in water are also discussed.

The final chapter summarizes the results of the studies and contributions to original knowledge. Some suggestions for future work are also included.

1.5 References

1. Stoenescu, R.; Meier, W. *Chem. Commun.* **2002**, 3016-3017.

2. Liu, F.; Eisenberg, A. *J. Am. Chem. Soc.* **2003**, 125(49), 15059-15064

3. Cotteril, R. *The Cambridge Guide to the Material World*, Cambridge University Press, **1985**, p. 215.

4. Cowie, J. M. G. *Polymers: Chemistry & Physics of Modern Materials* 2nd ed., Blackie Academic & Professional, New York, **1996**, p. 3-4.

5. Budd, Peter M. *J. Polym. Sci., Part B: Polym. Phys.* **1988**, 26(5), 1143-1147.

6. Cowie, J. M. G. *Polymers: Chemistry & Physics of Modern Materials* 2nd ed., Blackie Academic & Professional, New York, **1996**, p. 8-10.

7. O'Donnell, J. H.; Winzor, C. L.; Winzor, D. J. *Macromolecules* **1990**, 23(1), 167-172.

8. Cowie, J. M. G. *Polymers: Chemistry & Physics of Modern Materials* 2nd ed., Blackie Academic & Professional, New York, **1996**, p. 207-210.

9. Szwarc, M.; Beylen, M. V. *Ionic Polymerization and Living Polymers*, Chapman & Hall, New York, **1993**.

10. Hadjichristidis, N.; Pispas, S.; Floudas, G. *Block Copolymers : Synthetic Strategies, Physical Properties, and Applications*, Wiley, New York, **2003**.

11. Hsieh, H. L.; Quirk, R. P. eds. *Anionic Polymerization: Principles and Practical Applications*, Marcel Dekker, New York, **1996**.

12. Veregin, R. P. N.; Georges, M. K.; Kazmaier, P. M.; Hamer, G. K. *Macromolecules* **1993**, 26(20), 5316-20.

13. Patten, T. E.; Matyjaszewski, K. *Acc. Chem. Res.* **1999**, 32(10), 895-903.

14. Williams, D.; Flemming, I. *Spectroscopic Methods in Organic Chemistry, 4th ed.* McGraw-Hill Book Co., Montreal, **1987**.

15. Mitchell, T. N.; Costisella, B. *NMR-- from spectra to structures : an experimental approach*, Springer, Berlin, New York, **2004**.

16. Provder, T. ed., *Size Exclusion Chromatography: Methodology and Characterization of Polymers and Related Materials*, Washington DC, American Chemical Society, **1984**.

17. Matsen, M. W.; Bates, F. S. *J. Polym. Sci., Part B: Polym. Phys.* **1997**, 35(6), 945-952.

18. Matsen, M. W.; Schick, M. Phys. Rev. Lett. **1994**, 72(16), 2660-2663.

19. Hamley, I. W. J. Phys.: Condens. Matter **2001**, 13(33), R643-R671.

20. Schaz, A.; Lattermann, G. *Liq. Cryst.* **2005**, 32(4), 407-415.

21. Epps, T. H., III; Cochran, E. W.; Hardy, C. M.; Bailey, T. S.; Waletzko, R. S.; Bates, F. S. *Macromolecules* **2004**, 37(19), 7085-7088.

22. Zhang, L.; Eisenberg, A. *Polym. Adv. Technol.* **1998**, 9(10-11), 677-699.

23. Yu, Y.; Zhang, L.; Eisenberg, A. *Macromolecules* **1998**, 31(4), 1144-1154.

24. Halperin, A.; Tirrell, M.; Lodge, T. P. *Adv. Polym. Sci.* **1992**, 100, 31-37.

25. Zhang, L.; Eisenberg, A. *Science* **1995**, 268, 727-731.

26. Cameron, N. S.; Corbierre, M. K.; Eisenberg, A. *Can. J. Chem.* **1999**, 77(8), 1311-1326.

27. Yu, Y.; Eisenberg, A. *J. Am. Chem. Soc.* **1997**, 119, 8383-8384.

28. Yu, Y.; Zhang, L.; Eisenberg, A. *Macromolecules* **1998**, 31(4), 1144-1154.

29. Shen, H.; Eisenberg, A. *J. Phys. Chem. B* **1999**, 103(44), 9473-9487.

30. Zhang, L.; Eisenberg, A. *Polym. Adv. Technol.* **1998**, 9(10-11), 677-699.

31. Zhang, Lifeng; Eisenberg, Adi. *J. Am. Chem. Soc.* **1996**, 118(13), 3168-81.

32. Zhang, L.; Yu, K.; Eisenberg, A. *Science* **1996**, 272(5269), 1777-1779.

33. Zhang, L.; Eisenberg, A. *Macromolecules* **1996**, 29(27), 8805-8815.

34. Reimer, L. *Transmission Electron Microscopy Physics of Image Formation and Microanalysis, 4th ed,* Springer, Germany, **1997**.

35. van de Ven, T. G. M. *Colloidal hydrodynamics*, Academic Press, London, **1989**.

36. O'Brien, R. W.; White, L. R. *J. Chem. Soc. Faraday II* **1978**, *74*, 1607-1626.

Chapter 2

Synthesis and Characterization of PEO-*b*-PS-*b*-PAA Triblock Copolymers

2.1 Abstract

The synthesis of the PEO-*b*-PS-*b*-PAA triblock copolymers is based on atom transfer radical polymerization (ATRP), consisting of four major steps. First, a bromo-terminated PEO macro-initiator was prepared by the esterification of monomethoxy-capped PEO with 2-bromoisobutyryl bromide. The PEO macro-initiator was then used for the bulk ATRP of styrene catalyzed by CuBr/bipyridine to obtain the bromo-terminated PEO-*b*-PS diblock macro-initiator. Using the diblock macro-initiator and the catalyst system CuBr/*N,N,N',N',N''*-pentamethyldiethylenetriamine (PMDETA), the PEO-*b*-PS-*b*-P*t*BA parent triblock copolymers were synthesized by the ATRP of *t*-butyl acrylate (*t*-BA) in THF. The hydrolysis of the parent triblock copolymers mediated by trifluoroacetic acid produces the PEO-*b*-PS-*b*-PAA triblock copolymers. The hydrolysis of the *t*-BA groups was confirmed by IR. The compositions of the block copolymers were determined by ^{1}H NMR. The synthesized block polymers have relatively low polydispersity indexes (PDI < 1.3) as proved by GPC. The influence of several factors on the ATRP of styrene or *t*-BA, such as temperature, catalyst and polymerization time, was also explored.

2.2 Introduction

The synthesis of amphiphilic block copolymers with well-defined structures has been of increasing interest in polymer chemistry. Amphiphilic block copolymers can self-assemble in solution to form various aggregates, including spheres, rods, and vesicles. These self-assembled structures have potential applications in a variety of fields such as colloid science and biology. In the past decade, ABC-type triblock copolymers have attracted considerable interest due to the possibility to form new morphologies and interesting microdomain structures.[1-4] Recently, our interest has focused on the PEO-*b*-PS-*b*-PAA triblock copolymers, which have been employed successfully in the templated synthesis of CdS quantum dots located in the triblock copolymer aggregates.[5] The PEO-*b*-PS-*b*-PAA triblock copolymer vesicles with different corona chain compositions (PEO or PAA outside) may also serve as carriers for potential encapsulation applications.

The most widely used technique for the preparation of block copolymers has been anionic polymerization, involving in the sequential addition of different monomers. Although anionic polymerization is a powerful technique to synthesize block copolymers with well-defined structures, the types of monomers are limited and the polymerization is very sensitive to impurities. In addition, the order of monomer addition is restricted since the anion from the first monomer must be a stronger nucleophile than that from the second in order to initiate the second monomer.[6] The nucleophile reactivity of the anions formed from the monomers is generally in the following order: dienes, styrenes>vinylpyridines>(meth) acrylates>oxiranes>siloxanes. As a result, the polystyrene anion can react with either ethylene oxide (EO) or *t*-butyl acrylate (*t*-BA) to form more stable anions; however, neither EO anion nor *t*-BA anion can initiate styrene,

thus making impossible the preparation of PEO-*b*-PS-*b*-P*t*BA by sequential anionic polymerization.

The conventional free radical polymerization is tolerant for a wide range of monomers. However, for mixtures of monomers, copolymers with statistical compositions and relatively high polydispersity indexes are usually obtained. Due to the presence of chain termination reactions, the synthesis of well-defined block copolymers is impossible with free radical polymerization. In the last decade, two major controlled radical polymerization techniques based on reversible termination have been developed: stable free radical polymerization (SFRP) and atom transfer radical polymerization (ATRP). Since SFRP utilizes regular initiators for free radical polymerization, it is not applicable for the polymerization of ethylene oxide, and thus cannot be employed for the synthesis of PEO-*b*-PS-*b*-PAA triblock copolymers. By contrast, a block copolymer containing a PEO block can be prepared by ATRP using halogen-terminated PEO macro-initiators. ATRP is usually limited to monomers that do not strongly coordinate to the transition metal catalyst and is applicable to a wide range of monomers, including styrenes, acrylates, methacrylates, substituted acrylamides and acrylonitrile, although the polymerization of acrylic acid has not yet been successful.[7] Using ATRP, PEO-*b*-PS-*b*-PAA triblock copolymers with relatively low polydispersity indexes can be prepared through the hydrolysis of the PEO-*b*-PS-*b*-P*t*BA parent trilock copolymers.

Duxin *et al* first prepared the triblock copolymer PEO_{45}-*b*-PS_{150}-*b*-PAA_{108} with a long PAA block using ATRP.[5] In this thesis, the synthesis of PEO_{45}-*b*-PS_{156}-*b*-PAA_n with n=5, 15, 28 and 32, *i.e.*, much shorter PAA blocks, is reported. These materials are of interest in forming various morphologies, especially vesicles with different corona chain

compositions for potential encapsulation applications. The synthetic route is shown in Fig. 2.1. The synthesis consists of four major steps. First, a bromo-terminated PEO macro-initiator was prepared by the esterification of monomethoxy-capped PEO with 2-bromoisobutyryl bromide. The PEO macro-initiator was purified before use. The second step involves in the ATRP of styrene in bulk using the catalyst system CuBr/bipyridine (bpy). The resulting diblock macro-initiator was separated and purified before use. The third step is the ATRP of *t*-BA in THF to obtain the PEO-*b*-PS-*b*-P*t*BA parent triblock copolymers. The catalyst system is CuBr/*N,N,N',N',N''*-pentamethyldiethylenetriamine (PMDETA). Hydrolysis of the parent triblock copolymers mediated by trifluoroacetic acid yielded the PEO-*b*-PS-*b*-PAA triblock copolymers.

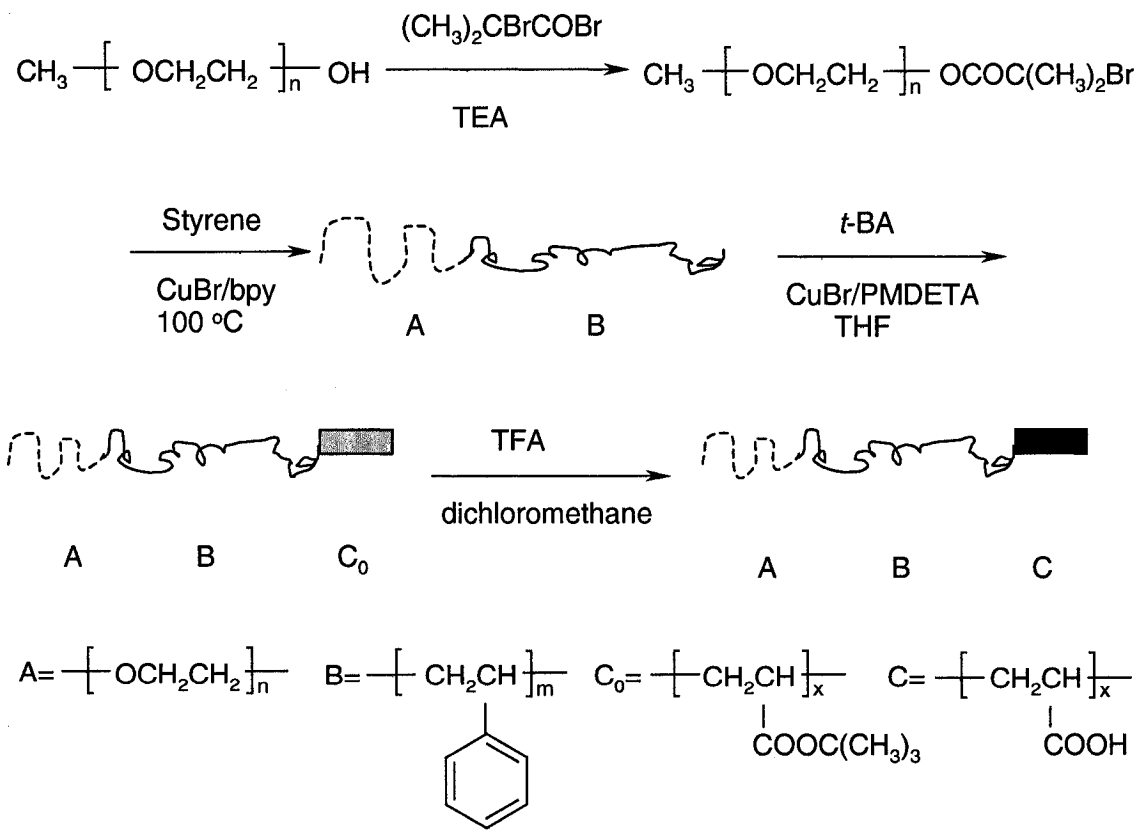

Fig. 2.1 Schematic of the synthesis of the PEO-*b*-PS-*b*-PAA triblock copolymers.

In the following sections, the synthesis of PEO-*b*-PS-*b*-PAA triblock copolymers is described in detail. The synthesized block copolymers have relatively narrow molecular weight distributions (M_w/M_n < 1.3) as proved by GPC, indicating that the polymerizations were controlled. The compositions of the block copolymers were determined by ^{1}H NMR. IR confirmed the hydrolysis of the *t*-BA groups. The influence of several factors on the ATRP of styrene or *t*-BA, such as temperature, catalyst and polymerization time, was also explored.

2.3 Experimental

2.3.1 Materials

All the chemicals were used without further purification unless otherwise stated. Tetrahydrofuran (THF) (99.5%), hexane (98.5%), and dichloromethane (99.5%) were purchased from EMD Chemicals. Triethylamine (TEA) (99%), benzene (99.9%), phosphorous pentoxide (P_2O_5) (99.1%) and methanol (99.9%) were purchased from Fisher Scientific. The following reagents were purchased from Aldrich: 2-Bromoisobutyryl bromide (98%), copper (I) bromide (CuBr) (98%), copper (II) bromide ($CuBr_2$) (98%), *N,N,N′,N″,N‴*-pentamethyldiethylenetriamine (PMDETA) (99%), styrene (99%), *t*-butyl acrylate (*t*-BA) (98%), 2,2-bipyridine (bpy) (99%), trifluoroacetic acid (TFA) (99%) and poly(ethylene glycol) methyl ether (PEO_{45}-OH) (M_n *ca.* 2000).

PEO_{45}-OH was vacuum dried overnight in the presence of P_2O_5 and stored under nitrogen at 0°C. Styrene and *t*-BA were dried over CaH_2 for 24 h, vacuum distilled, and then stored under nitrogen in the dark at -20°C. THF was purified by refluxing over

sodium benzophenone complex under nitrogen for several days (a blue-violet color indicating a solvent free of oxygen and moisture).

2.3.2 Synthesis of the PEO Macro-initiator

In a 500 mL two-neck flask, PEO_{45}-OH (10 g, 5.0 mmol) was dissolved in 250 mL THF, followed by the addition of triethylamine (1.4 mL, 10 mmol). The flask was then placed into an ice bath until it was cold. Then 2-bromoisobutyryl bromide (1.2 mL, 10 mmol) was added dropwise. After the addition was complete, the reaction mixture was allowed to warm to room temperature and stirred overnight. The white precipitate was removed by filtration and most of the THF in the clear filtrate was removed by rotary evaporation. The concentrated filtrate was then precipitated into excess ice-cold hexane. The resulting white powder was collected by filtration and then vacuum dried overnight in the presence of P_2O_5.

2.3.3 Synthesis of the Diblock Macro-initiator

For a typical bulk polymerization, the PEO macro-initiator (1.5 g, 0.70 mmol) was first vacuum dried in the presence of P_2O_5 for five hours in a 500 mL two-neck flask. The catalyst, CuBr (92.3 mg, 0.70 mmol) and bpy ligand (327 mg, 2.1 mmol) were then added together as solids under a slow nitrogen purge. Styrene (20 mL, 0.21 mol) was vacuum distilled for a second time before use. After the addition of styrene, a light-brown homogeneous solution was obtained under stirring. After three cycles of freeze-vacuum-thaw cycles, the flask was immersed into an oil bath at 100°C to start polymerization. After 16 h, a brown viscous mixture was obtained. The viscous mixture was exposed to

air, diluted with THF and then stirred for several hours. The green CuBr precipitate was removed by filtration and the brown filtrate was then precipitated into excess methanol. The resulting white powder was collected by filtration and vacuum dried overnight in the presence of P_2O_5.

2.3.4 Synthesis of the Parent Triblock Copolymers

A typical polymerization was performed as follows: the diblock macro-initiator (0.90 g, 0.050 mmol) was first dissolved in a small amount of benzene and then vacuum dried for five hours in a 500 mL two-neck flask. The catalyst CuBr (6.6 mg, 0.050 mmol) was then added under a slow nitrogen purge. The t-BA (3.16 mL, 20 mmol) was vacuum distilled for a second time before it was added to the flask, followed by the addition of THF (3.16 ml) as the solvent. The ligand, PMDETA (21 μL, 0.10 mmol) was finally added via an airtight microsyringe. The resulting light-green solution was degassed by three freeze-vacuum-thaw cycles. The flask was then immersed into an oil bath at 60°C to start polymerization. After 3 h, the light-green polymer solution was exposed to air to stop the polymerization. The green CuBr precipitate was removed by filtration. The light-green filtrate was diluted with THF and then precipitated into excess methanol. The resulting white powder was collected by filtration and then vacuum dried overnight in the presence of P_2O_5.

2.3.5 Hydrolysis of the Parent Triblock Copolymers

The parent triblock copolymer (1.0 g) was first dissolved in 25 mL dichloromethane in a 50 mL reaction flask. The TFA (6.0 equiv to the *t*-butyl acrylate

groups) was then added dropwise under stirring. After the addition of the TFA was complete, the flask was immersed into an oil bath at 40°C and the solution was refluxed overnight. The dichloromethane and excess TFA were then removed by rotary evaporation. The resulting light-brown glassy solid was dissolved in THF and then precipitated into excess water. A white powder was obtained by filtration and then vacuum dried overnight in the presence of P_2O_5.

2.3.6 Characterization

The IR spectra of the polymers were obtained on a Perkin Elmer 16PC Fourier-Transform Infrared Spectrophotometer. Samples were prepared by first dissolving the polymers in chloroform and then casting polymer films on KBr windows. The IR spectra were recorded over a frequency range of 4000-400 cm^{-1}.

The ^1H NMR spectra of the polymers were obtained at 25°C on a Varian 300-MHz instrument. The sample solutions were prepared by dissolving the polymers in $CDCl_3$. Copolymer compositions were calculated from the integrals of the proton peaks.

Molecular weights and molecular weight distributions were determined on a GPC system consisting of a Waters 410 pump, a guard column (Waters Styragel), two columns (Waters Styragel HR4 and HR1, with a separation performance ranging from 1×10^2 to 6×10^5 g/mol) and a Varian RI-4 refractive index detector. Measurements were performed using THF as the eluent with a flow rate of 0.6 mL/min at 26°C. The column system was calibrated using a set of linear monodisperse polystyrene standards.

2.4 Results and Discussion

2.4.1 Synthesis of the PEO Macro-initiator

The PEO macro-initiator was prepared through the esterification reaction between the monomethoxy-capped PEO and 2-bromoisobutyryl bromide. The chemical structure of the PEO macro-initiator was characterized by IR and ^{1}H NMR.

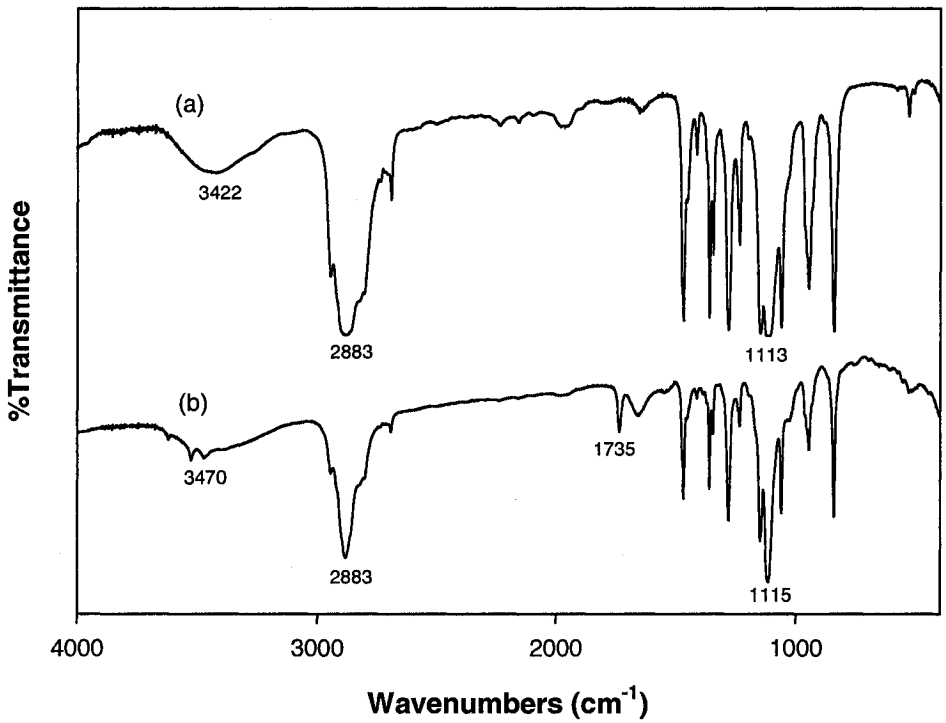

Fig. 2.2 FTIR spectra of (a) monomethoxy-capped PEO and (b) the PEO macro-initiator.

The FT-IR spectra of the monomethoxy-capped PEO and the PEO macro-initiator are shown in Fig. 2.2. In the spectrum of the monomethoxy-capped PEO (a), typical absorptions can be observed at 3420 (O-H stretching of the hydroxyl end groups), 2883

(C-H stretching) and 1113 cm^{-1} (C-O-C stretching).[8-9] The formation of the PEO macro-initiator was confirmed by comparing its IR spectrum with that of the monomethoxy-capped PEO. In the spectrum of the PEO macro-initiator (b), an absorption peak at 1735 cm^{-1} was observed, attributed to the C=O stretching of the ester groups. However, the IR results are not precise enough to prove the complete conversion of all the hydroxyl end groups of the monomethoxy-capped PEO, due to the existence of a broad O-H stretching peak at 3470 cm^{-1}. The presence of the broad peak could be due to either the incomplete esterification reaction or the attracted moisture because PEO is hygroscopic.

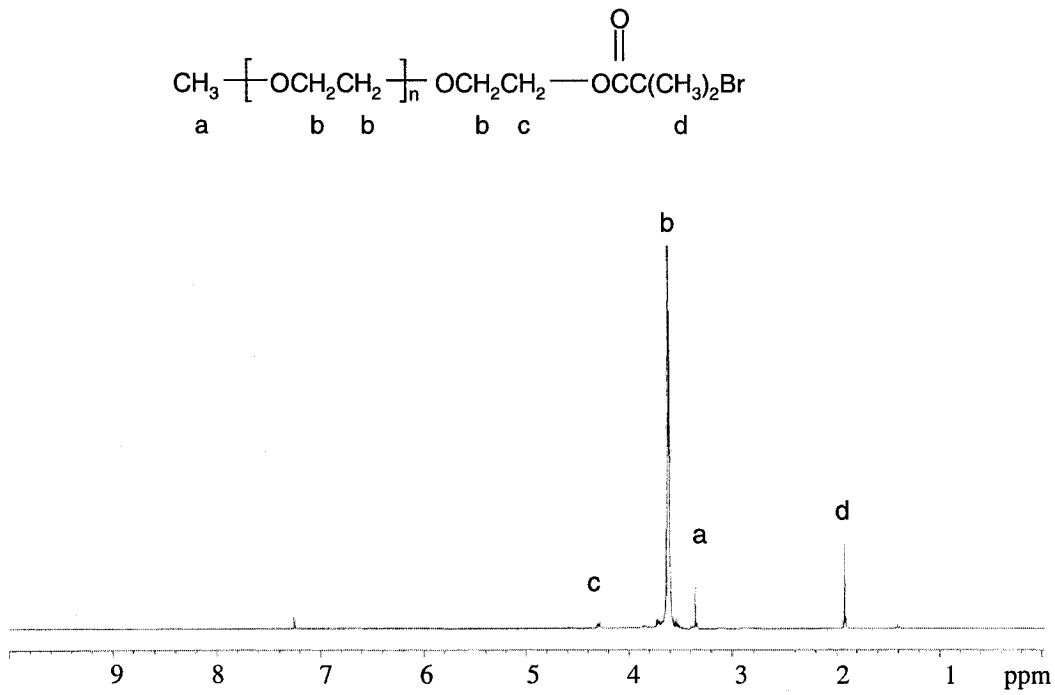

Fig. 2.3 ^{1}H NMR spectrum of the PEO-Br macro-initiator.

^{1}H NMR is useful to confirm the complete substitution of the hydroxyl end groups of the monomethoxy-capped PEO. The ^{1}H NMR spectrum of the PEO macro-initiator is shown in Fig. 2.3; the peaks can be assigned as follows: δ= 1.94 (d, 6H), 3.38

(a, 3H), 3.60 (b, 180H), 4.33 (c, 2H). The characteristic peak of the hydroxyl end groups of PEO at around 2.45 ppm disappeared and two new signals presented at 4.33 (c) and 1.94 ppm (d), resulting from the substituted PEO.[10]

The molecular weight and molecular weight distribution of the PEO macro-initiator were determined by GPC. The GPC chromatograph showed a narrow unimodal peak as can be seen from Fig. 2.4 (a). The GPC traces of the diblock macro-initiator and the parent triblock copolymer are also included in this figure and will be discussed later.

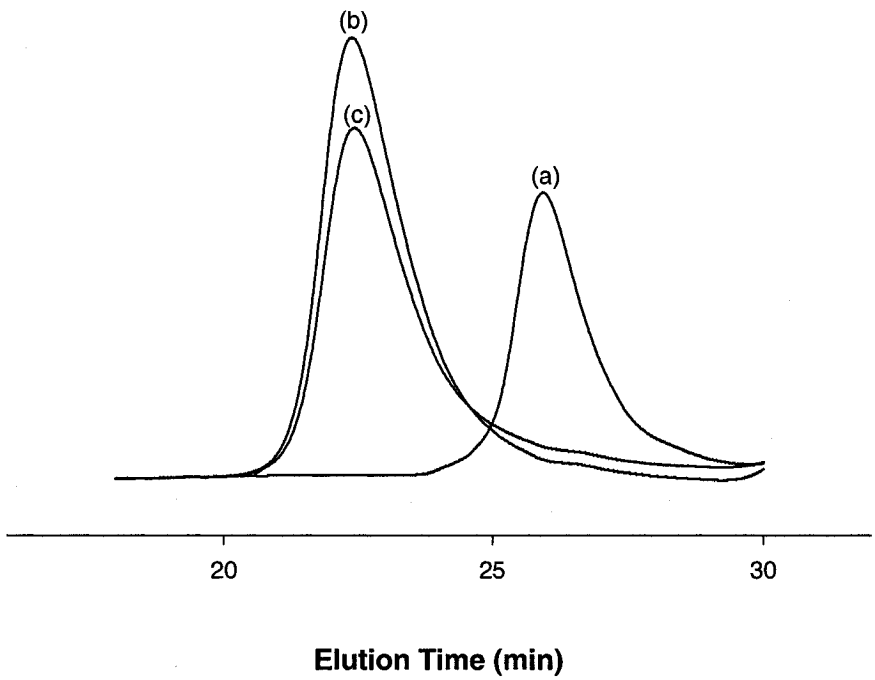

Fig. 2.4 GPC traces of (a) the PEO macro-initiator, (b) the diblock macro-initiator and (c) the parent triblock copolymer.

2.4.2 Synthesis of the Diblock Macro-initiator

The diblock macro-initiators were synthesized through bulk ATRP of styrene using the bromo-terminated PEO macro-initiator. Fig. 2.5 shows a representative FTIR spectrum of the diblock copolymers. The peaks can be assigned as follows: the peak at 1110 cm^{-1} is due to the C-O-C stretching of the PEO block and the peak at 2924 cm^{-1} results from the sp^3 C-H stretching; the peak at 3026 cm^{-1} is characteristic of the sp^2 C-H stretching of benzene rings, and the peaks at 1601, 1493 and 1453 cm^{-1} are attributed to the aromatic C-C bending vibrations[11], thus confirming the formation of the PEO-*b*-PS-Br diblock macro-initiator. In addition, the strong peaks at 758 and 699 cm^{-1} are characteristic of monosubstituted benzenes.

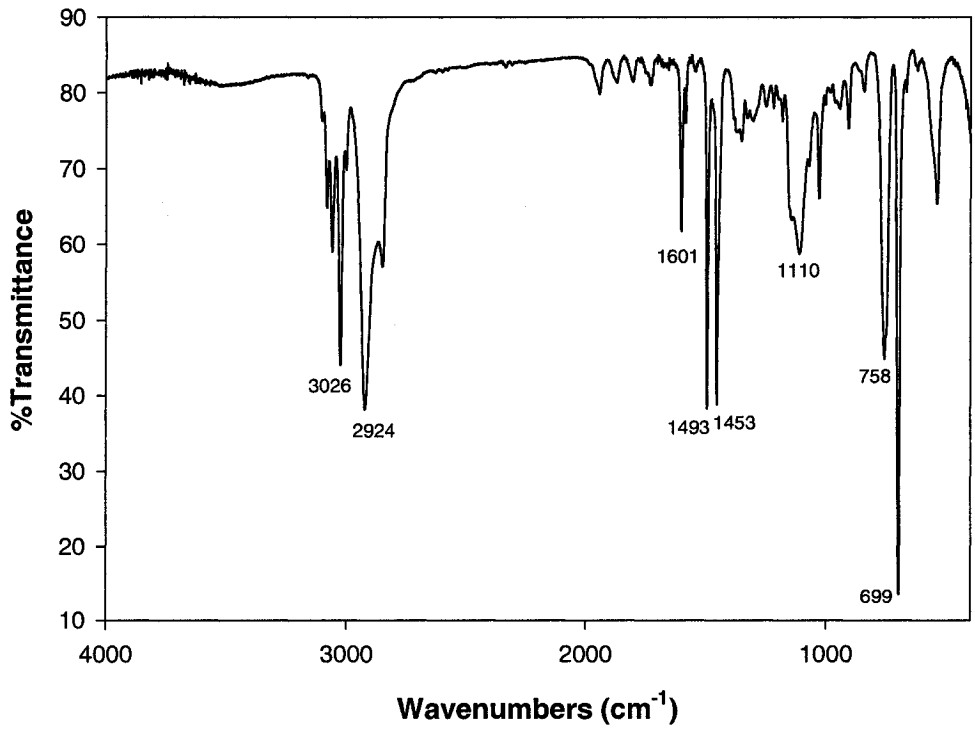

Fig. 2.5 A representative FTIR spectrum of the PEO-*b*-PS-Br diblock macro-initiator.

The average block length of polystyrene was further determined by ^{1}H NMR. A typical ^{1}H NMR spectrum is shown in Fig. 2.6. The peak at 3.65 ppm is characteristic of the PEO block (OCH_2CH_2), and the resonance signals at 6.28-7.45 ppm are typical of phenyl rings, also establishing the successful synthesis of the diblock macro-initiator. The monomethoxy-capped PEO was purchased from Aldrich and the number of the repeating unit is *ca.* 45. Since the block length of PEO is known, the average block length of PS can be calculated using the integral value of the signals due to phenyl rings.

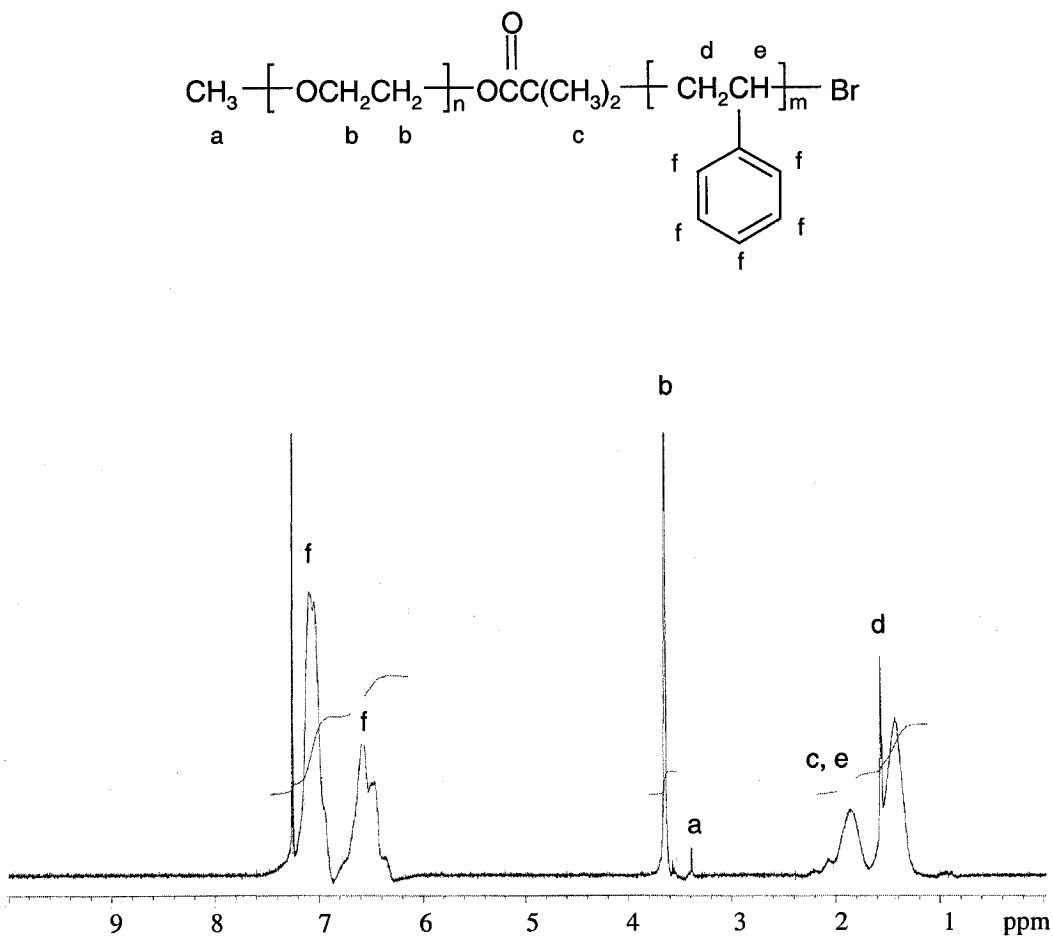

Fig. 2.6 A typical ^{1}H NMR spectrum of the PEO-*b*-PS-Br diblock macro-initiator.

The molecular weights and molecular weight distributions of the two diblock macro-initiators were determined by GPC and the results are shown in Table. 2.1. The polydispersity indexes were relatively low, indicating that the polymerizations were controlled. The molecular parameters and the preparatory conditions of the parent triblock copolymers are also included and will be discussed later. A unimodal distribution of the diblock initiator was also observed as illustrated in Fig. 2.4, suggesting the absence of homo-polystyrene and the PEO macro-initiator.

Table 2.1 Molecular weights [a] and polydispersity indexes [b] of the macro-initiators and the parent triblock copolymers prepared under different conditions.

Sample	M_n *ca.*	M_w/M_n	Polymerization Temperature (°C)	Polymerization Time (h)	Catalyst System (molar ratio)
PEO-Br	2,200	1.13			
PEO_{45}-*b*-PS_{156}-Br	18,400	1.23	100	16	CuBr/bpy (1/3)
PEO_{45}-*b*-PS_{178}-Br	20,700	1.29	100	24	CuBr/bpy (1/3)
PEO_{45}-*b*-PS_{156}-*b*-P*t*BA_5	19,000	1.30	60	3	CuBr/$CuBr_2$/PMDETA (1/0.1/2)
PEO_{45}-*b*-PS_{156}-*b*-P*t*BA_{15}	20,300	1.28	60	3	CuBr/$CuBr_2$/PMDETA (1/0.05/2)
PEO_{45}-*b*-PS_{156}-*b*-P*t*BA_{28}	22,000	1.24	60	3	CuBr/PMDETA (1/2)
PEO_{45}-*b*-PS_{156}-*b*-P*t*BA_{32}	22,500	1.28	75	3	CuBr/PMDETA (1/2)

[a] Molecular weights were calculated according to ^{1}H NMR compositions. [b] Polysispersity indexes were determined by GPC.

2.4.3 Synthesis of the Parent Triblock Copolymers

2.4.3.1 Characterization of the Parent Triblock Copolymers

The PEO-*b*-PS-*b*-P*t*BA parent triblock copolymers were prepared by the ATRP of *t*-BA in THF employing the diblock macro-initiator. The structures of the triblock copolymers were characterized by IR and ^{1}H NMR. A typical FTIR spectrum of PEO-*b*-PS-*b*-P*t*BA parent trilock copolymers is given in Fig. 2.7. The appearance of peaks at 1729 (C=O stretching of *t*-BA), 1367 and 1148 (C-O stretching of *t*-BA) cm^{-1},[12-13] besides the characteristic peaks for PEO and PS blocks as discussed in section 2.4.2, confirms the formation of the PEO-*b*-PS-*b*-P*t*BA triblock copolymer.

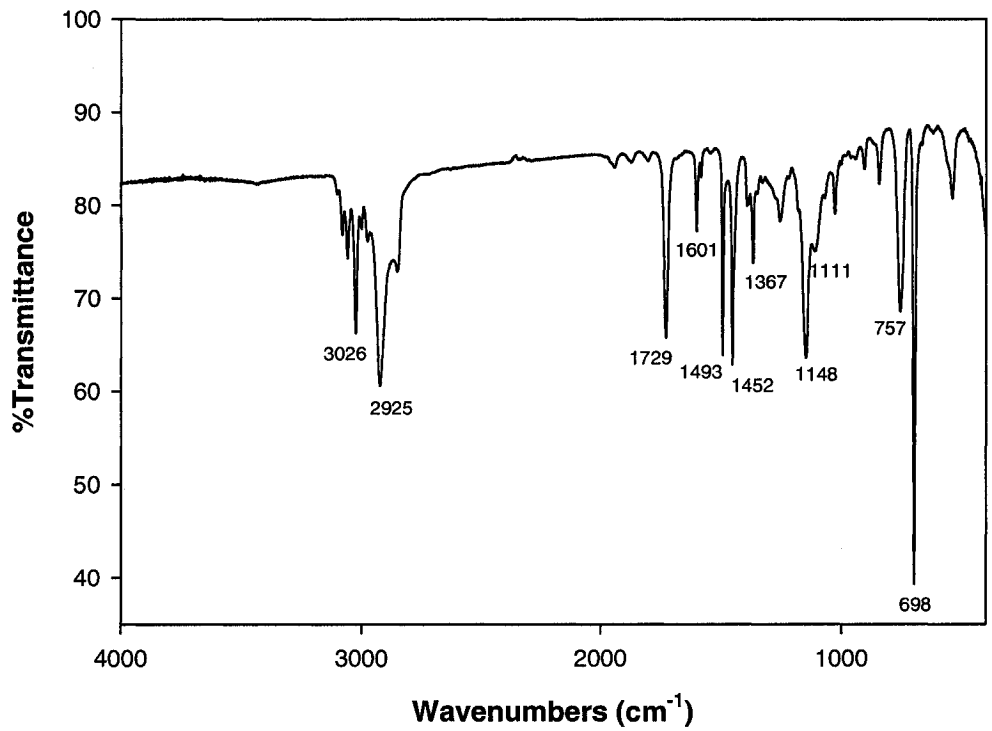

Fig. 2.7 A representative FTIR spectrum of PEO-*b*-PS-*b*-P*t*BA.

In the ^{1}H NMR spectrum (Fig. 2.8), the presence of P*t*BA block cannot be evidenced from the characteristic peak of the methyl groups (i) of *t*-BA since the signal of the methyl groups overlaps with those of the aliphatic methylene groups (d and g). Nevertheless, the increased integral of the peak area between 1.15 and 2.32 ppm, plus the proton signals of PEO and PS as described in section 2.4.2, further proves the existence of the PEO-*b*-PS-*b*-P*t*BA triblock copolymer. The compositions of the triblock copolymers were calculated from the integrals of the proton peaks.

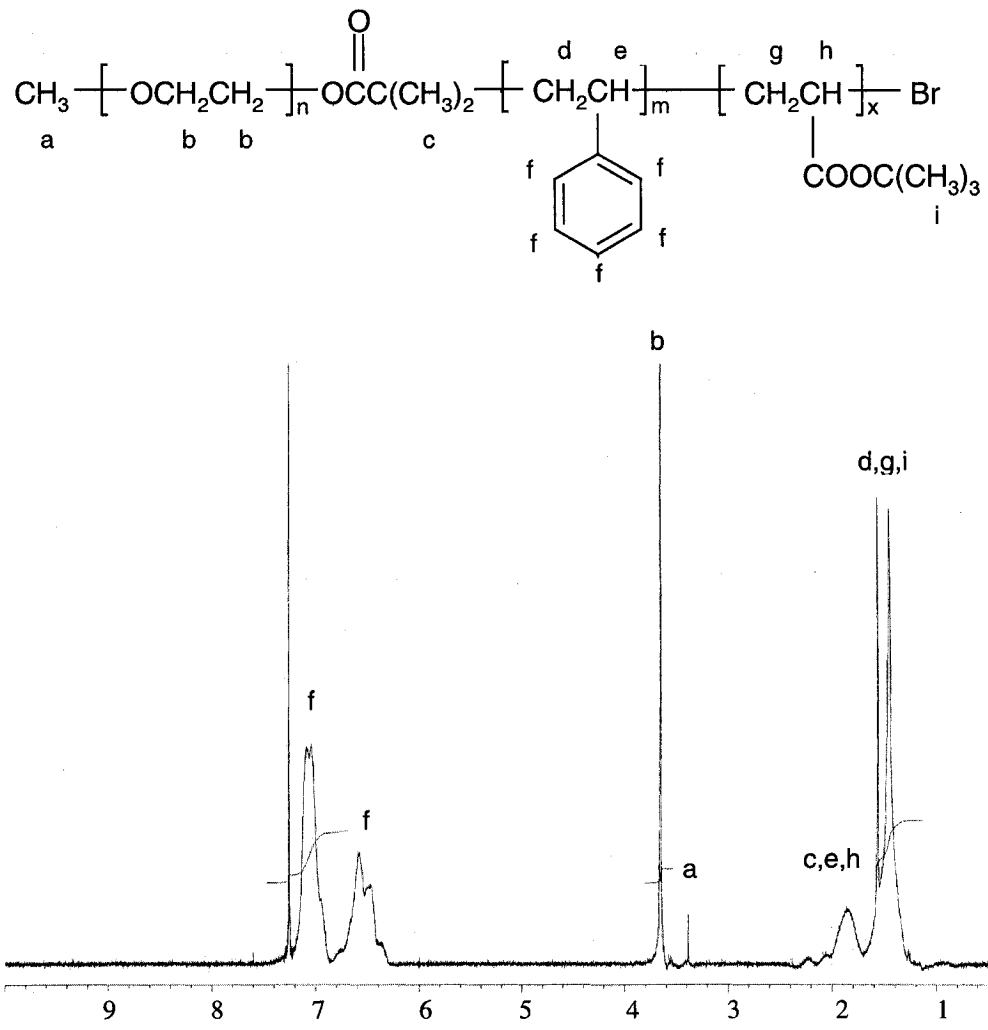

Fig. 2.8 A typical ^{1}H NMR spectrum of PEO-*b*-PS-*b*-P*t*BA parent triblock copolymers.

The molecular weights and molecular weight distributions of the parent triblock copolymers were determined by GPC. In Table 2.1, the molecular weights were calculated according to the ^{1}H NMR compositions since GPC results were unreliable. For example, the molecular weights of the triblock copolymers were always lower than that of the diblock macro-initiator, which could be ascribed to the difference in hydrodynamic properties of the copolymers and the polystyrene standards used in the calibration. Nevertheless, GPC is useful to determine the polydispersity indexes (M_w/M_n) of the polymers.

The GPC chromatographs of the macro-initiators and the parent triblock copolymer are presented in Fig. 2.4. As is evident, the macro-initiators and the parent triblock copolymer have unimodal distributions. As can be seen from Table 2.1, the polydispersity indexes of the copolymers are a little higher than that of the PEO-Br macro-initiator, but are still considerably lower than the value of 2.0 typical of regular free radical polymerization, confirming that the polymerizations were controlled.

2.4.3.2 Effect of Polymerization Time on the ATRP of Styrene

The average length of PS block and the polydispersity index increased slightly as the polymerization time increased. After sixteen hours of polymerization, a diblock copolymer with a PS block length of 156 (PDI: 1.23) was prepared, while Duxin *et al* achieved a PS block length of 150 (PDI: 1.12) after twelve hours of polymerization.[5] By increasing the polymerization time to one day, the average length of PS block increased to 178; the polydispersity index also increased slightly to 1.29.

As is well established, there is a linear relationship between the degree of polymerization and the polymerization time for a living polymerization. Assuming that the polymerizations of styrene were living, the expected block length of PS would be [M]/[I]=300. As can be seen from Table 2.1, the block length of PS reached 156 after sixteen hours of polymerization, *i.e.*, 52% styrene was consumed; after one day's polymerization, the block length of PS increased slightly to 178, *i.e.*, about 59% styrene was utilized. The nonlinear increase of molecular weight of PS block as a function of time is probably due to the slow kinetics at high viscosity since the polymerizations were performed in bulk. Reining *et al* observed a phase separation during the bulk ATRP of styrene with a PEO macro-initiator at 130°C and attributed the relatively lower conversion of styrene to the incompatibility of the PEO macro-initiator and styrene.[14] However, no such phase separation was observed for the bulk ATRP of styrene at 100°C in our research.

Consequently, a PEO-*b*-PS diblock macro-initiator with a much longer PS block and relatively low polydispersity is not likely to be prepared by simply increasing the polymerization time. More active PEO macro-initiators or catalyst systems may be used to prepare a diblock macro-initiator with a much longer PS block.

2.4.3.3 Effect of Catalyst and Temperature on the ATRP of *t*-BA

The catalyst system has a significant effect on the ATRP of *t*-BA. Triblock copolymers with different average block lengths of P*t*BA can be synthesized by adjusting the amount of $CuBr_2$ in the CuBr/$CuBr_2$/PMDETA catalyst system. As shown in Table 2.1, a triblock copolymer with an average P*t*BA block length of 28 was prepared at 60°C

without the addition of $CuBr_2$. At a Cu (I)/Cu (II) molar ratio of 1/0.1, the P*t*BA block length significantly decreased to 5. A triblock copolymer with an intermediate P*t*BA block length of 15 was synthesized by varying the Cu (I)/ Cu (II) molar ratio to 1/0.05. As described in previous chapter, the ATRP mechanism involves a reversible switching between two oxidation states of the transition metal complex. The activator is typically a Cu (I) halide complex, while the Cu (II) halide complex acts as a deactivator to reduce the concentration of radicals through a deactivation process in order to achieve a controlled polymerization. Therefore, the addition of Cu (II) species reduces the overall rate of ATRP due to an increased rate of deactivation.[15-18] In addition, the presence of Cu (II) species reduces the concentration of active Cu (I) species, resulting in a decrease of the apparent rate constant of activation and possible dramatic decrease of the overall rate of ATRP.[18-19]

The temperature also affects the ATRP. Ma *et al*[20] have found that the temperature has a significant effect on the bulk ATRP of *t*-BA catalyzed by CuBr/PMDETA. The polymerizations were controlled at a temperature of 50°C. However, at higher temperatures such as 90°C, the polymerization was rapid (the reaction mixture solidified in less than 10 min), and the polydispersity was broad (PDI: 2). By contrast, in our research on the ATRP of *t*-BA in THF, no major temperature effect was found. As indicated in Table 2.1, the average length of P*t*BA block slightly increased from 28 to 32 as the temperature changed from 60°C to 75°C. The polydispersity remained relatively low (PDI: 1.28) and the GPC chromatograph showed a unimodal peak, indicating that the polymerization was controlled.

2.4.4 Hydrolysis of the Parent Triblock Copolymers

After the relative block length of P*t*BA was known, the P*t*BA block of the parent triblock copolymer was converted to PAA through the hydrolysis reaction mediated by an excess of trifluoroacetic acid in dichloromethane. The removal of the *t*-butyl groups was confirmed by IR. A typical FTIR spectrum of PEO-*b*-PS-*b*-PAA triblock copolymers is given in Fig. 2.9. In the spectrum, the complete removal of all the *t*-butyl groups is evidenced from the disappearance of the characteristic peaks of *t*-BA at 1729, 1367 and 1148 cm^{-1}. Furthermore, the existence of carboxylic acids is indicated by the appearance of a broad band at 1734 cm^{-1} which is characteristic of the C=O stretching of the carboxylic acid groups.[12-13]

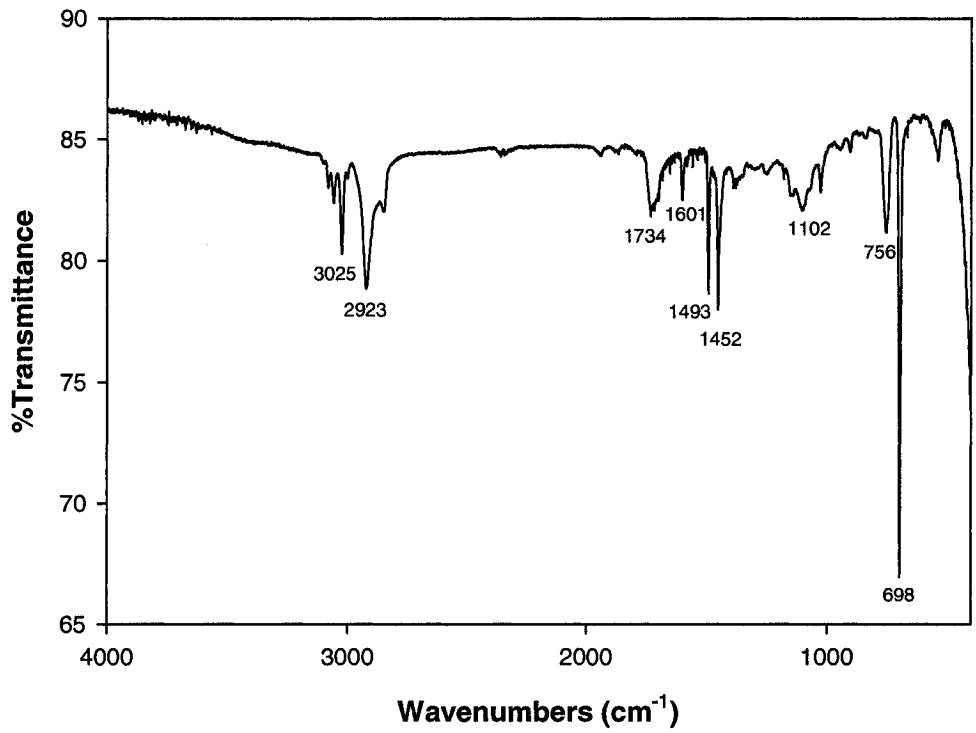

Fig. 2.9 A representative FTIR spectrum of PEO-*b*-PS-*b*-PAA.

2.5 Conclusions

PEO-*b*-PS-*b*-PAA triblock copolymers with different PAA block lengths were successfully synthesized using ATRP technique in four major steps. IR and ^{1}H NMR measurements confirmed the formation of the macro-initiators and the triblock copolymers. The compositions of the copolymers were calculated from the integrals of the proton peaks in the ^{1}H NMR spectra. GPC yielded unreliable molecular weights for the PEO-containing polymers due to the difference in hydrodynamic properties of the polymers and the polystyrene standards used in the calibration, so the molecular weights were calculated according to compositions determined by ^{1}H NMR. Nevertheless, GPC is useful to determine the polydispersity indexes of the polymers. The GPC chromatographs of the macro-initiators and the parent triblock copolymer show unimodal peaks. In addition, the polydispersity indexes of all the copolymers are relatively low (M_w/M_n < 1.3), indicating that the polymerizations were controlled. The average length of PS block and polydispersity index gradually increased as the polymerization time increased. The average length of P*t*BA block can be adjusted by varying the amount of $CuBr_2$ in the catalyst system. Unlike the bulk ATRP of *t*-BA,[20] no significant effect of temperature was found. The average length of P*t*BA block increased slightly from 28 to 32 as the temperature increased from 60°C to 75°C but the polydispersity remained relatively low.

2.6 References

1. Krappe, U.; Stadler, R.; Voigt-Martin, I. *Macromolecules* **1995**, 28(13), 4558-4561.
2. Brinkmann, S.; Stadler, R.; Thomas, E. L. *Macromolecules* **1998**, 31(19), 6566-6572.
3. Stoenescu, R.; Meier, W. *Chem. Commun.* **2002**, 3016-3017.

4. Liu, F.; Eisenberg, A. *J. Am. Chem. Soc.* **2003**, 125, 15059-15064.

5. Duxin, N.; Liu, F.; Vali, H.; Eisenberg, A. *J. Am. Chem. Soc.* **2005**, 127(28), 10063- 10069.

6. Cowie, J. M. G. *Polymers: Chemistry & Physics of Modern Materials* 2nd ed., Blackie -Academic & Professional, New York, **1996**, p.97-100.

7. Patten, T. E.; Matyjaszewski, K. *Acc. Chem. Res.* **1999**, 32(10), 895-903.

8. Williams, D.; Flemming, I. *Spectroscopic Methods in Organic Chemistry, 4th ed.* McGraw-Hill Book Co., Montreal, **1987**.

9. Krishnan, R.; Srinivasan, K. S. V. *Eur. Polym. J.* **2003**, 39, 205-210.

10. Sun, X.; Zhang, H.; Huang, X.; Wang, X.; Zhou, Q.-F. *Polymer* **2005**, 46(14), 5251-5257.

11. Lu, Z.; Chen, S.; Huang, J. *Macromol. Rapid Commun.* **1999**, 20, 394-400.

12. Cameron, N. S.; Eisenberg, A.; Brown, G. R. *Biomacromolecules* **2002**, 3, 116-123.

13. Terreau, O. L. *Ph. D. Thesis*, McGill University, **2004,** p.181-182.

14. Reining, B.; Keul, H.; Hocker, H. *Polymer* **1999**, 40, 3555-3563.

15. Matyjaszewski, K.; Patten, T. E.; Xia, J. *J. Am. Chem. Soc.* **1997**, 119, 674-680.

16. Wang, J. L.; Grimaud, T.; Matyjaszewski, K. *Macromolecules* **1997**, 30, 6507-6512.

17. Davis, K. A.; Paik, H.-j.; Matyjaszewski, K. *Macromolecules* **1999**, 32, 1767-1776.

18. Matyjaszewski, K.; Nanda, A. K.; Tang W. *Macromolecules* **2005,** 38, 2015-2018.

19. Yoshikawa, C.; Goto, A.; Fukuda, T. *Macromolecules* **2003**, 36, 908-912.

20. Ma, Q.; Wooley, K. L. *J. Polym. Sci. Part A: Polym. Chem.* **2000**, 38, 4805-4820.

Chapter 3

Multiple Morphologies of PEO-*b*-PS-*b*-PAA Triblock Copolymers in Solution

3.1 Abstract

The self-assembly of PEO-*b*-PS-*b*-PAA triblock copolymers into different morphologies is described in this chapter. The effects of several factors on the aggregate size and morphology are discussed, including the nature and compositions of the common solvent, PAA block length, pH, water content and initial copolymer concentration. Multiple morphologies, including spheres, vesicles, lamellae and rods, were prepared by varying the above factors and studied by TEM. The mechanisms of the morphological or size changes of the aggregates under different conditions are also discussed.

3.2 Introduction

Amphiphilic block copolymers, like small surfactants, can self-assemble into micelles or aggregates in selective solvents.[1-8] In a polar solvent, regular micelles with a hydrophobic core and a hydrophilic corona are formed, while in a solvent of low polarity, reverse micelles with the opposite structure are made. Depending on the relative length of the corona block, micelles can be further divided into two categories: star-like micelles with much longer corona chains, and crew-cut aggregates that have much shorter corona chains compared with the size of the core chains.[2]

The self-assembly of asymmetric amphiphilic diblock copolymers has received extensive attention in the past decade. One important aspect of crew-cut aggregates is that a wide variety of aggregate morphologies can be prepared. Besides simple spheres, many other morphologies have been observed, such as rods, vesicles, lamellae, large compound micelles (LCMs), bicontinuous rods and other structures.[9] In 1995, Zhang and Eisenberg first reported the systematic preparation of crew-cut aggregates with various morphologies from PS-*b*-PAA diblock copolymers.[5] In our group, multiple morphologies have also been observed in solutions of other diblock copolymer families, including PS-*b*-PEO,[10-12] PBD-*b*-PAA,[13] and PS-*b*-P4VP.[14] Other groups also investigated the self-assembly of different diblock copolymers, including the group of Discher,[15] who prepared giant vesicles from polyethylene oxide-*b*-polyethylethylene. The giant vesicles were proved to be almost an order of magnitude tougher than typical phospholipids. The group of Bates[16] reported the formation of vesicles, wormlike micelles and complex morphologies such as Y-junctions and three-dimensional networks from poly (*1,2*-butadiene-*b*-ethyleneoxide) in dilute aqueous solutions.

For the asymmetric amphiphiles with long hydrophobic blocks, the aggregates cannot be prepared by directly dissolving the copolymers in water. Instead, the copolymers are first dissolved in a common solvent that is good for both hydrophilic and hydrophobic blocks, followed by the addition of a precipitant such as water to induce self-assembly. At a critical water concentration (CWC), micellization occurs and the copolymers undergo a transition from free chains to micelles. A further increase in the water content may induce morphological transitions. The aggregates are quenched in excess water to kinetically freeze their cores and maintain the morphologies. Subsequent dialysis against water removes the organic solvent.

The formation of different morphologies is determined by a balance among three factors: the corona-chain repulsion, the core-chain stretching and the interfacial tension between the micelle core and the outside solution.[5] Thus, parameters that affect the above balance can be used to control the formation of various aggregate morphologies. A wide range of parameters have been used to control the size and morphology of the aggregates prepared from diblock copolymers, including copolymer composition, water content, nature and composition of the common solvent, different additives and other factors.[17]

In contrast to the extensive studies on the aggregate morphologies of diblock copolymers in solution, only a few publications described the solution properties of ABC-type triblock copolymers. Patrickios's group[18] investigated the effect of block sequence on the micellization of ABC triblock copolymers with two hydrophilic blocks and a hydrophobic block, namely 2-(dimethylamino)ethyl methacrylate, hexa(ethylene glycol) methacrylate or methacrylic acid, and methyl methacrylate. They synthesized three block sequence isomers, ABC, ACB and BAC and determined hydrodynamic

diameters of the resulting micelles in water. The small micelle size around 10 nm suggests the formation of spheres. The interesting fact is that the micelle sizes of the triblock copolymers with a hydrophobic midblock are approximately one half of those of the other two isomers. Kriz *et al.*[19] reported the formation of core-shell-shell spherical micelles from poly(2-ethylhexyl acrylate)-*b*-poly(methyl methacrylate)-*b*-poly(acrylic acid) in THF/water. Yu and Eisenberg[7] observed multiple morphologies from PS_{180}-*b*-$PMMA_{67}$-*b*-PAA_{37} by varying the solvent or water content. Spheres and rods were obtained at a water content of 18% w/w in dioxane, and vesicles were prepared when the water content increased to 25% w/w. In THF, LCMs and spheres were made at a water content of 40% w/w. A necklace structure was found in DMF at 55% w/w added water. Müller's group[20] studied the solution properties of a triblock copolyampholyte, poly(5-(N, N-dimethylamino) isoprene)-*b*-polystyrene-*b*-poly(methacrylic acid) in THF/water and found large vesicles with pH-independent radii around 100 nm. Recently, Meier's group[21] reported the preparation of vesicles with asymmetric membrane structures from an ABC-type triblock copolymer, poly(ethylene oxide)-*b*-poly(dimethylsiloxane)-*b*-poly(2-methyloxazoline) with two hydrophilic blocks separated by a hydrophobic midblock. Their results support the thermodynamic stabilization mechanism of block copolymer vesicles previously proposed by Luo and Eisenberg[22], stating that the short hydrophilic blocks preferentially segregate to the inside of the vesicles and the long hydrophilic blocks to the outside. Liu and Eisenberg[23] studied the effect of pH on the morphology of a new type of ABC triblock copolymer, poly(acrylic acid)-*b*-polystyrene-*b*-poly(4-vinyl pyridine). Vesicles with P4VP outside were prepared at low apparent pH (pH*=1), while at pH*14, vesicles with PAA outside were obtained; at intermediate pH*,

spheres and short rods were found. Most interestingly, vesicles with PAA outside can be inverted to P4VP outside by changing pH under dynamic conditions.

In this chapter, we report on a detailed study of the aggregate morphology of a new type of ABC triblock copolymer, PEO-*b*-PS-*b*-PAA, with a nonionic hydrophilic PEO block and an ionizable PAA block separated by a hydrophobic PS block. The effects of several factors on the self-assembly of the triblock copolymers in solution were explored. In particular, we studied the aggregate morphologies using different solution conditions, including the nature and composition of the common solvent, pH, the water content in the solvent mixture and the initial copolymer concentration. Multiple morphologies including spheres, rods, lamellae and vesicles were prepared by varying the above conditions. The morphological transitions or size changes under different conditions are explained in terms of the force balance of the three main contributions to the free energy of micellization: the core-chain stretching, the corona-chain repulsion, and the interfacial tension between the micelle core and the outside solution.

3.3 Experimental

3.3.1 Materials

Three triblock copolymer samples were used in this study. The molecular parameters of the polymers are listed in Table 3.1. The details of synthesis and characterization of the triblock copolymers were presented in chapter two. All the triblock copolymers have relatively narrow and unimodal molecular weight distributions. The composition and polydispersity of each triblock copolymer were determined by ^{1}HNMR and GPC, respectively. 1,4-dioxane (dioxane, purity 99.0%), N, N-dimethyl

formamide (DMF, purity 99.9%) and tetrahydrofuran (THF, purity 99.5%) were purchased from Fisher Scientific. NaOH and HCl standard solutions (0.1004 and 0.0959 N, respectively) were purchased from Aldrich. Milli-Q water (18.2 MΩ cm resistivity) was used in all of the experiments. If not mentioned otherwise, all materials were used as received.

Table. 3.1 Molecular Characteristics of the PEO-*b*-PS-*b*-PAA Triblock Copolymers.

Polymer [a]	PAA content (mol %)	M_w/M_n [b]
PEO_{45}-*b*-PS_{156}-*b*-PAA_5	2.4	1.30
PEO_{45}-*b*-PS_{156}-*b*-PAA_{15}	6.9	1.28
PEO_{45}-*b*-PS_{156}-*b*-PAA_{28}	12.2	1.24

[a] Polymer compositions were determined by ^{1}H NMR. [b] Polydispersity indexes of the polymers were measured by GPC in the form of PEO-*b*-PS-*b*-P*t*BA.

3.3.2 Aggregate Preparation

A desired amount of each triblock copolymer was dissolved in a common solvent (dioxane, DMF or THF) or in solvent mixtures and stirred overnight to obtain a homogeneous solution. To induce self-assembly, Milli-Q water was added dropwise to each solution at a rate of *ca.* 0.25% (w/w) per minute to the desired final concentration. The samples were then quenched by adding them dropwise into excess water while stirring vigorously. Finally, the samples were dialyzed against Milli-Q water for three days to remove the organic solvents. To study the effect of additives (HCl or NaOH), an

aqueous solution containing a certain amount of the additive instead of Milli-Q water was added and the aggregate solutions were prepared by the same procedure as described above.

3.3.3 Aggregate Characterization

3.3.3.1 Turbidity Measurements

A Varian Cary 50 UV-Vis spectrophotometer was used to measure the solution turbidity at room temperature. Absorbance readings were recorded using a wavelength of 650 nm. At this wavelength, both the free chains and the aggregates of the triblock copolymers have minimal absorption, therefore the attenuation of light is due to the scattering of light by the aggregates.

3.3.3.2 pH Measurements

The pH measurements were performed using an Oaklon 510 pH/mV/Temperature meter at 25°C. The pH meter was calibrated with standard pH buffers (pH 4.00, 7.00, and 10.00). A certain amount of HCl or NaOH aqueous solution was added dropwise to the triblock copolymer in dioxane, and the pH value of the colloid solution was recorded. The pH values were measured in a mixture of dioxane and water and are reported as the apparent pH (pH*).

3.3.3.3 Transmission Electron Microscopy (TEM)

A JEOL JEM-2000 FX electron microscope operating at an acceleration voltage of 80 keV was used to examine the morphologies of the samples. To prepare samples for

TEM, 10 μL of a dialyzed aggregate solution was deposited on a copper grid coated first with a thin film of Formvar and then with carbon. The copper grids containing sample droplets were left to air-dry overnight. TEM pictures were taken with a multi-scan CCD camera. The average sizes of the aggregates were determined by Sigma Scan Pro 4.0 software. Three hundred vesicles or spheres were counted to obtain the average size.

3.4 Results and Discussion

3.4.1 Effect of the Nature and Composition of the Common Solvent

The nature and composition of the common solvent used to dissolve the block copolymer are factors that control the formation of different aggregate morphologies. The onset of micellization and possible subsequent morphological changes were monitored by measuring the turbidity of 1.0% (w/w) PEO_{45}-*b*-PS_{156}-*b*-PAA_{28} solutions in dioxane, THF and DMF as a function of water content. As presented in Fig. 3.1, the turbidity diagrams of the copolymer in dioxane and THF show a single jump at a water content of 19% (w/w) and 38% (w/w), respectively. This jump is associated with the transition from single chains to aggregates. However, no visible transition occurred for the triblock copolymer in DMF with water contents up to 60% (w/w). The solution was always transparent and the turbidity remained the same. It is possible that the copolymer concentration is lower than the CMC even at a water content of 60% (w/w). Another possibility is that the triblock copolymer molecules could form monomolecular micelles in DMF/water. Sadron[24] was the first to use the term "monomolecular micelle". He assumed that the molecules of an amphiphilic diblock copolymer in a very dilute solution of a selective solvent would form monomolecular micelles with an insoluble core and a

swollen soluble shell; by increasing the concentration of the copolymer, polymolecular micelles, such as spheres, rods and vesicles, would form.

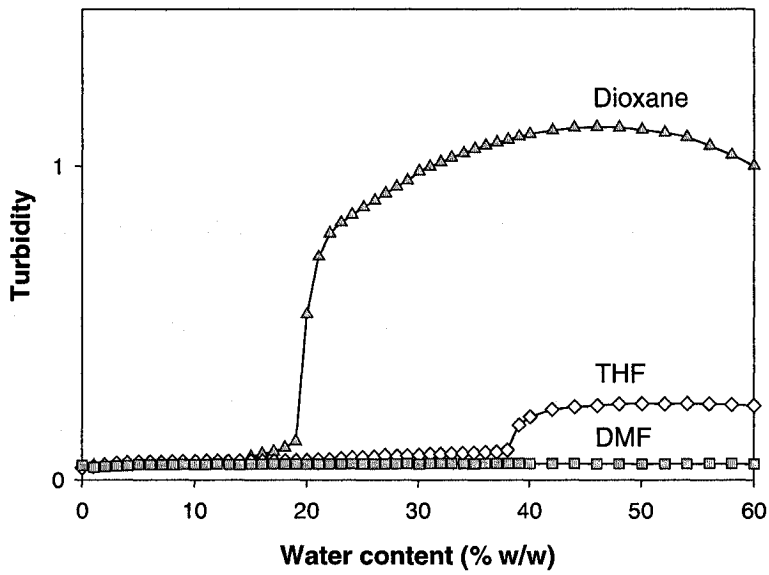

Fig. 3. 1 Turbidity diagrams of 1.0% (w/w) solutions of PEO_{45}-*b*-PS_{156}-*b*-PAA_{28} in dioxane, THF, and DMF.

For the 1.0% (w/w) triblock copolymer in DMF, the quality of the solvent becomes worse with the continued addition of water. The molecules of the triblock copolymer may undergo micro-separation of the blocks, with the hydrophobic PS block collapsing into a small core and the hydrophilic PEO and PAA blocks forming the swollen soluble shell. The schematic of the triblock copolymer monomolecular micelle is given in Fig. 3.2. The PEO blocks form loops extending out into solution, providing steric stabilization; the acrylic acid groups of the PAA block are partially ionized, electrostatically stabilizing the monomolecular micelle. The solvated swollen shell would be capable of protecting the insoluble core and thus preventing further association. The

size of the monomolecular micelles in DMF/water would be smaller than that of the random coils in DMF. This speculation may be further proved by small angle neutron scattering (SANS).

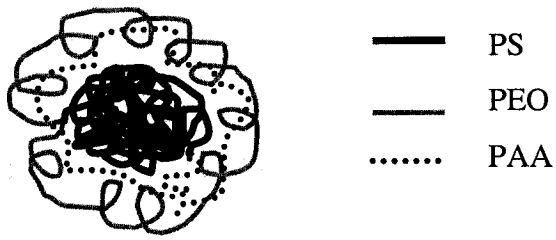

Fig. 3.2 Schematic of a monomolecular micelle of 1.0% (w/w) PEO_{45}-*b*-PS_{156}-*b*-PAA_{28} in DMF/water.

Mixtures of solvents were also used to study whether a progressive change in the nature of the common solvent would be accompanied by gradual changes in the aggregate morphology. The morphologies of the aggregates formed from solutions of 1.0% (w/w) PEO_{45}-*b*-PS_{156}-*b*-PAA_{28} in THF, dioxane and their mixtures at a water content of 60% (w/w) are shown in Fig. 3.3. In THF, spheres of uniform size (33 $\pm$ 4 nm) are observed. In dioxane, vesicles with an average outside diameter of 82 $\pm$ 27 nm are seen and a few spheres are also present. In solvent mixtures of THF and dioxane, the percentage of spheres decreases and the average size of vesicles slightly increases as the content of dioxane increases. The average thickness of the vesicle walls remains the same and is very uniform, at *ca.* 15 nm.

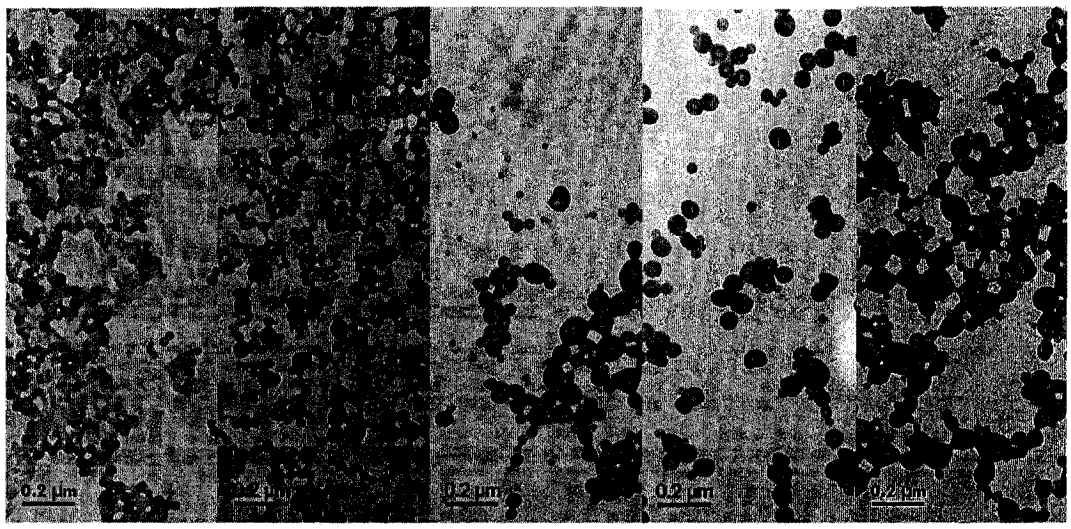

THF/dioxane	1/0	3/1	1/1	1/3	0/1
Avg. Diam.	33 ± 4 nm	56 ± 11 nm	55 ± 18 nm	65 ± 9 nm	82 ± 27 nm

Fig. 3.3 TEM images of aggregates prepared from 1.0% (w/w) PEO_{45}-*b*-PS_{156}-*b*-PAA_{28} in solvent mixtures of THF and dioxane at different weight ratios at a water content of 60% (w/w).

The morphologies of the aggregates formed from solutions of 1.0% (w/w) PEO_{45}-*b*-PS_{156}-*b*-PAA_{28} in dioxane and the mixtures of DMF and dioxane at a water content of 60% (w/w) are shown in Fig. 3.4. In DMF, no aggregates were found, supporting the result of turbidity measurement that excludes the formation of polymolecular micelles. As can be seen from Fig. 3.4, the addition of DMF has a significant effect on the aggregate morphology. In a solvent mixture of 25% w/w DMF and 75% w/w dioxane, spheres (26 ± 3 nm) are dominant, though several small vesicles are also present. By adding 10% w/w DMF in the solvent mixture, the average size of the vesicles considerably decreases by 30 nm and more spherical micelles are seen. The results described above illustrate the significant effect of the nature and composition of the

common solvent on the aggregate morphology. Since spheres are observed in THF and no aggregate morphology in DMF, dioxane may be the best solvent for generating multiple morphologies.

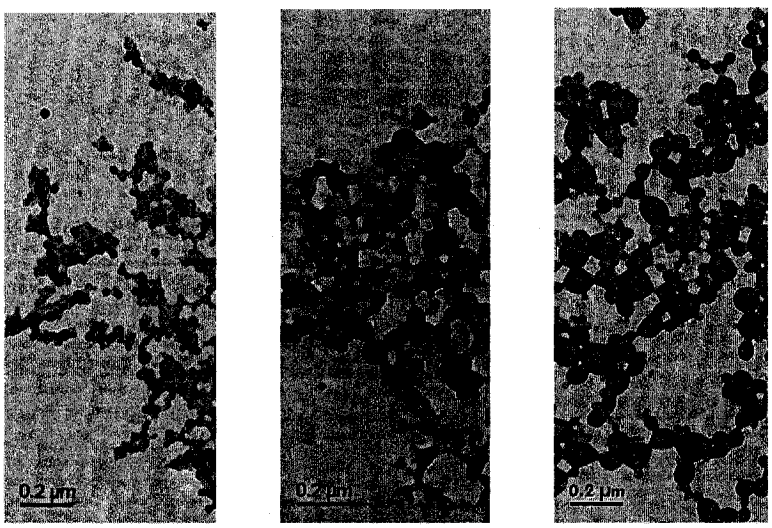

DMF/dioxane	**1/3**	**1/9**	**0/1**
Avg. Diam.	**26 ± 3 nm**	**52 ± 10 nm**	**82 ± 27 nm**

Fig. 3.4 TEM images of aggregates prepared from 1.0% (w/w) PEO_{45}-*b*-PS_{156}-*b*-PAA_{28} in solvent mixtures of DMF and dioxane at different weight ratios at a water content of 60% (w/w).

The formation of spheres in THF and vesicles in dioxane is controlled by the polymer-solvent interactions. The interactions between the PS core and the solvent can be estimated by comparing the solubility parameter of homo-PS with those of the solvents, while the dielectric constants of the solvents can be used to estimate the degree of corona chain repulsion, as suggested by Yu and Eisenberg.[25] The solubility parameter of homo-PS is 16.6-20.2 $[Mpa]^{1/2}$.[25] As can be seen from Table 3.2,[25] the solubility parameter of

THF is closer to that of homo-PS than that of dioxane. So the solvent content in the PS core is higher in THF, resulting in a higher degree of core chain stretching. Since the dielectric constant of THF is higher than that of dioxane, a higher degree of ionization of acrylic acid groups is expected in THF, leading to a higher degree of corona chain repulsion. A higher degree of core stretching favors the formation of bigger aggregates other than spheres, while a higher degree of corona chain repulsion facilitates the formation of spheres. The corona chain repulsion must be the dominant force, so a final morphology of spheres in THF and vesicles in dioxane is obtained, respectively.

Table. 3.2 Dielectric constants (ε) and solubility parameters (δ) of dioxane, THF, and DMF.[25]

Solvent	ε	$\delta([\text{MPa}]^{1/2})$
dioxane	2.2	20.5
THF	7.5	18.6
DMF	38.2	24.8

It is of interest to compare the CWC values of the triblock copolymer with those of PS-*b*-PAA diblock copolymers in different solvents. The CWC values of the diblock copolymers with a relatively long PS block are about 5% (w/w) in DMF, 10% (w/w) in dioxane and 18% (w/w) in THF.[26] For the diblock copolymers, the CWC is mainly determined by the solubility of the hydrophobic PS block. As discussed above, the solubility parameter of homo-PS is the closest to that of THF and the farthest from that of DMF. Therefore, the solubility of PS block is the highest in THF and the lowest in DMF. Consequently, the CWC is the lowest in DMF and the highest in THF. For the triblock

copolymer PEO_{45}-*b*-PS_{156}-*b*-PAA_{28}, the CWC is not the lowest in DMF since no aggregates are formed and the CWC values are higher in dioxane (19% w/w) and in THF (38% w/w) compared with those of the diblock copolymers. This is probably because the self-assembly of the triblock copolymer is mainly determined by the corona chain repulsion. The dielectric constant of DMF is the highest as shown in Table 3.2, so the corona chain repulsion is the highest in DMF since more acrylic acid groups are ionized in that solvent than in the others, making the self-assembly the most difficult to occur. In addition, the PEO block may provide steric stabilization, making the association of the hydrophobic blocks more difficult.

3.4.2 Effect of PAA Block Length

The PAA block length has a significant effect on the vesicle size as shown in Fig. 3.5. Under the same preparatory conditions, large vesicles with an average size of 433 $\pm$ 155 nm were prepared from PEO_{45}-*b*-PS_{156}-*b*-PAA_5; by contrast, small vesicles with an average size of 82 $\pm$ 27 nm and a few spheres were obtained from PEO_{45}-*b*-PS_{156}-*b*-PAA_{28}, while vesicles with an intermediate average size 336 $\pm$ 132 nm were found for PEO_{45}-*b*-PS_{156}-*b*-PAA_{15}. The average wall thickness of PEO_{45}-*b*-PS_{156}-*b*-PAA_5 vesicles is significantly bigger than those of PEO_{45}-*b*-PS_{156}-*b*-PAA_{15} and PEO_{45}-*b*-PS_{156}-*b*-PAA_{28} vesicles. It should be noted that the PEO_{45}-*b*-PS_{156}-*b*-PAA_{15} vesicles are collapsed as shown in the TEM image. Therefore, the average wall thickness should be one half of that measured directly from the images of the vesicles.

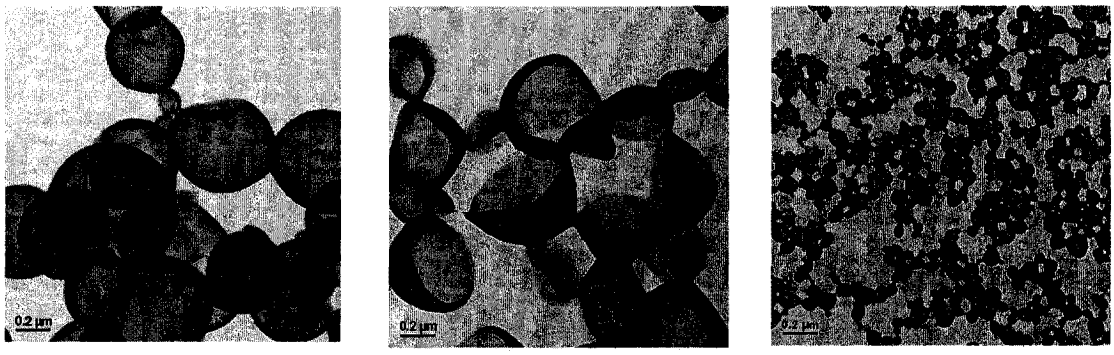

PEO_{45}-*b*-PS_{156}-*b*-PAA_5	PEO_{45}-*b*-PS_{156}-*b*-PAA_{15}	PEO_{45}-*b*-PS_{156}-*b*-PAA_{28}
Avg. Diam=433 ± 155 nm	**Avg. Diam= 336 ± 132 nm**	**Avg. Diam=82 ± 27 nm**
Avg. Wall Thick=22 ± 3 nm	**Avg. Wall Thick= 13 ± 2 nm**	**Avg. Wall Thick=14 ± 2 nm**

Fig. 3.5 TEM images of aggregates prepared from 1.0% (w/w) PEO_{45}-*b*-PS_{156}-*b*-PAA_5, PEO_{45}-*b*-PS_{156}-*b*-PAA_{15}, and PEO_{45}-*b*-PS_{156}-*b*-PAA_{28} in dioxane at a water content of 60% (w/w).

The increasing corona chain repulsion is responsible for the decrease of vesicle size with increasing PAA block length. As the corona chain repulsion increases, the radius of curvature becomes smaller, resulting in smaller vesicles, as suggested by Choucair *et al.*[27] The external corona chain compositions of the vesicles can be determined qualitatively by comparing the zeta-potential curves of the vesicles with those of PS-*b*-PEO and PS-*b*-PAA vesicles, which will be discussed in detail in Chapter 4.

3.4.3 Effect of pH

pH affects the aggregate morphology since acrylic acid is pH responsive. The aggregate morphologies of PEO_{45}-*b*-PS_{156}-*b*-PAA_{28}, formed under different apparent pH (pH*) conditions with an initial copolymer concentration of 1.0% w/w in dioxane are

shown in Figure 3.6. With increasing pH*, the aggregate morphology changes from vesicles at pH*1 and pH*5 to lamellae and short rods at pH*13 (molar ratio of NaOH/AA, R = 0.092). The vesicles prepared at pH*1 have an average outside diameter of 192 ± 98 nm, while for those prepared at pH*5, the comparable value is 82 ± 27 nm. The vesicles prepared at pH*1 are collapsed as shown in Fig. 3.6, therefore the vesicle wall thickness (14 ± 3 nm) is actually the same as that of the vesicles prepared at pH*5 (14 ± 2 nm).

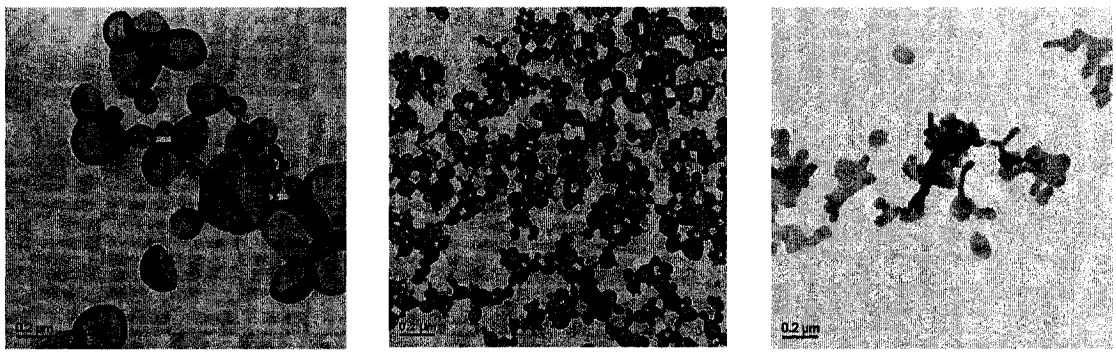

pH*1 **pH*5** **pH*13**

Fig. 3.6 TEM images of aggregates prepared from 1.0% (w/w) PEO_{45}-*b*-PS_{156}-*b*-PAA_{28} in dioxane at a water content of 60% (w/w) at different pH*.

The size and morphological changes are mainly controlled by the varied degree of corona chain repulsion under different pH. At low pH, the degree of ionization of acrylic acid groups is low, and thus the repulsive interactions among the PAA chains are low. By contrast, at high pH, more acrylic acid groups are ionized, leading to a higher degree of repulsion among PAA chains. As the pH* changes from 1 to 5, the corona chain repulsion increases, favoring the formation of smaller vesicles due to the decrease of the

radius of curvature.[27] As the pH* further increases to 13, the corona chain repulsion increases significantly, leading to the conversion of vesicles into small lamellae and rods.

3.4.4 Effect of Water Content

The water content also has an effect on the aggregate morphologies. As discussed in Section 3.4.1, the CWC for 1.0% (w/w) PEO_{45}-*b*-PS_{156}-*b*-PAA_{28} in dioxane is 19% w/w. As the water content increases above CWC, a transition from single chains to aggregates occurs.

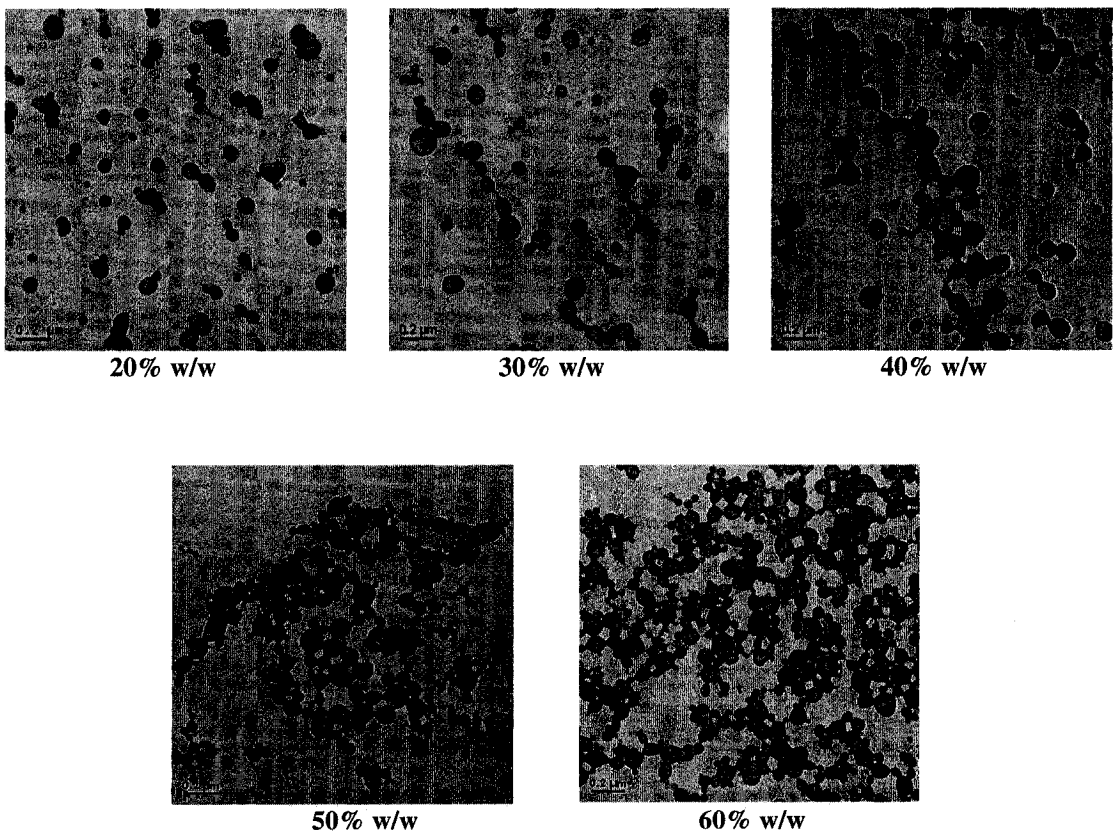

Fig. 3.7 TEM images of aggregates prepared from 1.0% (w/w) PEO_{45}-*b*-PS_{156}-*b*-PAA_{28} in dioxane at different water contents.

As shown in Fig. 3.7, vesicles, spheres and large compound micelles coexist at a relatively low water content of 20% w/w; while at the water content ranging from 30% to 60% w/w, vesicles are prevalent. However, the average diameter and wall thickness of the vesicles remain almost the same at water contents ranging from 30% w/w to 60% w/w.

The effect of water content on the vesicle size is a balance of the effects of the interfacial energy and the corona chain repulsion.[27] As the water content increases, both the interfacial energy and the corona chain repulsion increase. However, the increasing interfacial energy favors the formation of bigger vesicles, while the increasing corona chain repulsion facilitates the formation of smaller vesicles. Since no change occurs to the average size of the vesicles, the two effects must conteract.

3.4.5 Effect of Initial Copolymer Concentration

It was of interest to see to what extent the initial copolymer concentration could be used to control the aggregate size and morphology. As shown in Fig. 3.8, vesicles are found for all the initial copolymer concentrations. The average size of the vesicles increases slightly with the increasing initial copolymer concentration, while the average wall thickness of the vesicles remains almost the same.

The effect of the initial copolymer concentration is related to its effect on the aggregation number. The higher the initial copolymer concentration, the higher the aggregation number. As the initial copolymer concentration increases, the aggregation number also increases, leading to bigger vesicles.

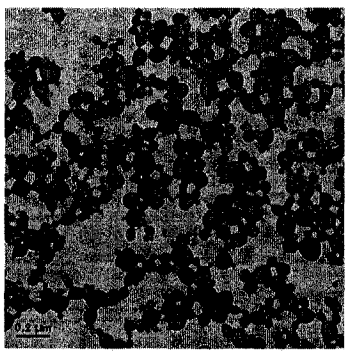

1.0% w/w

Avg. Diam=82 ± 27 nm
Avg. Wall Thick=14 ± 2 nm

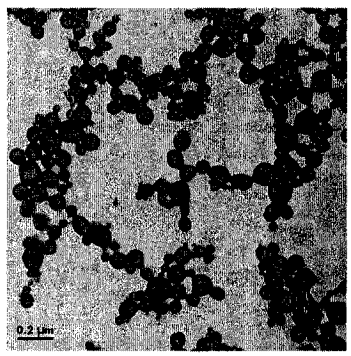

1.5% w/w

Avg. Diam=85 ± 27 nm
Avg. Wall Thick=15 ± 2 nm

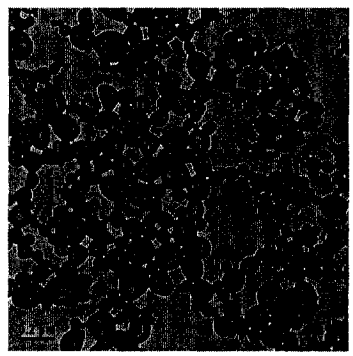

2.0% w/w

Avg. Diam=100 ± 36 nm
Avg. Wall Thick=14 ± 4 nm

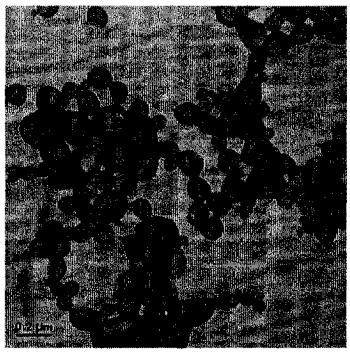

2.5% w/w

Avg. Diam=116 ± 37 nm
Avg. Wall Thick=15 ± 4 nm

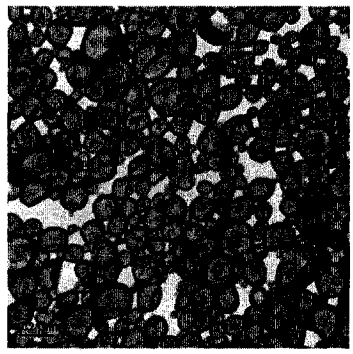

3.0% w/w

Avg. Diam=120 ± 44 nm
Avg. Wall Thick=15 ± 3 nm

Fig. 3.8 TEM images of aggregates prepared from PEO_{45}-*b*-PS_{156}-*b*-PAA_{28} in dioxane with different initial copolymer concentrations at the water content of 60% (w/w).

3.5 Conclusions

The triblock copolymer PEO-*b*-PS-*b*-PAA, with a long hydrophobic PS block and relative short hydrophilic PEO and PAA blocks, can form aggregates with multiple

morphologies under various preparatory conditions. The effects of different factors on the aggregate size and morphology were investigated.

The solvent has a significant effect on the aggregate morphologies. No aggregates were found in DMF, while spheres were prepared in THF and vesicles were obtained in dioxane. This is probably because the micellization is mainly controlled by the corona chain repulsion. The degree of corona chain repulsion is related to the dielectric constants (ε) of the solvents. The ε values of DMF, THF and dioxane are 38.2, 7.5 and 2.2, respectively.[25] The corona chain repulsion is highest in DMF since more acrylic acid groups are ionized due to its highest dielectric constant. Although no aggregates were seen in DMF, monomolecular micelles with a compact insoluble PS core may have formed. In addition, the PEO may also provide steric stabilization of the monomolecular micelles, further preventing the formation of polymolecular aggregates. The corona chain repulsion is lower in THF than in DMF, so the single chains start to aggregate into spherical micelles. In dioxane, the corona chain repulsion is the lowest and vesicles are found.

Solvent mixtures of THF/dioxane and DMF/dioxane have also been used to study whether a progressive change in the nature of the common solvent would be accompanied by gradual changes in the aggregate morphology. As the content of THF or DMF increases, more spheres tend to form and the size of vesicles decreases. DMF has a more significant effect than THF. By adding 25% w/w DMF to the solvent mixture, only spheres were found, while both vesicles and spheres were present with the same content of THF in the solvent mixture.

The PAA block length has a significant effect on the vesicle size. This is mainly due to the varied corona chain repulsion with different PAA block lengths. With a shorter PAA block length, the corona chain repulsion is lower, resulting in the formation of bigger vesicles due to the increasing radius of curvature.[27]

The pH also influences the aggregate size and morphology. At the apparent pH (pH*) of 1, big vesicles with an average diameter of 192 $\pm$ 98 nm are observed, while at pH*5, smaller vesicles with an average diameter of 82 $\pm$ 27 nm are found. At pH*13, small lamellae and rods are seen. The decrease of the vesicle size is due to the increasing corona chain repulsion with the increasing pH.[27] The corona chain repulsion becomes bigger at higher pH since more acrylic acid groups are ionized. As the pH* changes from 5 to 13, the corona chain repulsion increases significantly, leading to the conversion of vesicles into small lamellae and rods.

The effect of water content on the vesicle size is a balance of the effects of the interfacial energy and the corona chain repulsion.[27] As the water content increases, both the interfacial energy and the corona chain repulsion increase. However, the increasing interfacial energy favors the formation of bigger vesicles, while the increasing corona corona chain repulsion. Since no change occurs to the average size of the vesicles, the two effects must conteract.

The initial copolymer concentration also affects the vesicle size. The average size of vesicles increases slightly from 82 $\pm$ 27 to 122 $\pm$ 44 nm as the initial copolymer concentrations increases from 1.0% w/w to 3.0% w/w. This is probably due to the increasing aggregation number with the increasing initial copolymer concentration.

3.6 References

1. Tuzar, Z.; Kratochvil, P. *Adv. Colloid Interface Sci.* **1976**, 6, 201-232.
2. Halperin, A.; Tirrell, M.; Lodge, T. P. *Adv. Polym. Sci.* **1992**, 100, 31-37.
3. Desjardens, A.; van de Ven, T. G. M.; Eisenberg, A. *Macromolecules* **1992**, 25, 2412-2421.
4. Gao, Z.; Varshney, S. K.; Wong, S.; Eisenberg, A. *Macromolecules* **1994**, 27, 7923-7927.
5. Zhang, L.; Eisenberg, A. *Science* **1995**, 268, 727-731.
6. Zhang, L.; Eisenberg, A. *J. Am. Chem. Soc.* **1996**, 118, 3168-3181.
7. Yu, G. E.; Eisenberg, A. *Macromolecules* **1998**, 31, 5546-5549.
8. Liu, F.; Eisenberg, A. *J. Am. Chem. Soc.* **2003**, 125, 15059-15064.
9. Cameron, N. S.; Corbierre, M. K.; Eisenberg, A. *Can. J. Chem.* **1999**, 77(8), 1311-1326.
10. Yu, K.; Eisenberg, A. *Macromolecules* **1996**, 29(19), 6359-6361.
11. Yu, K.; Zhang, L.; Eisenberg, A. *Langmuir* **1996**, 12(25), 5980-5984.
12. Yu, K.; Eisenberg, A. *Macromolecules* **1998**, 31(11), 3509-3518.
13. Yu, Y.; Zhang, L.; Eisenberg, A. *Langmuir* **1997**, 13(9), 2578-2581.
14. Shen, H.; Zhang, L.; Eisenberg, A. *J. Am. Chem. Soc.* **1999**, 121(12), 2728-2740.
15. Discher, B. M.; Won, Y.-Y.; Ege, D. S.; Lee, J. C.-M.; Bates, F. S.; Discher, D. E.; Hammer, D. A. *Science* **1999**, 284(5417), 1143-1146.
16. Jain, S.; Bates, F. S. *Science* **2003**, 300, 460-446.

17. Choucair, A.; Eisenberg, *A. Eur. Phys. J. E.* **2003**, 10, 37-44.

18. (a) Patrickios, C. S.; Lowe, A. B.; Armes, S. P.; Billingham, N. C. *J. Polym. Sci., Part A: Polym. Chem.* **1998**, 36(4), 617-631. (b) Triftaridou, A. I.; Vamvakaki, M.; Patrickios, C. S.; Lue, L. *Macromol. Symp.* **2002**, 183, 133-138. (c) Triftaridou, A. I.; Vamvakaki, M.; Patrickios, C. S. *Polymer* **2002**, 43(10), 2921-2926.

19. Kriz, J.; Masar, B.; Plestil, J.; Tuzar, Z.; Pospisil, H.; Doskocilova, D. *Macromolecules* **1998**, 31(1), 41-51.

20. Bieringer, R.; Abetz, V.; Müller, A. H. E. *Eur. Phys. J.* **2001**, E5, 5-12.

21. Stoenescu, R.; Meier, W. *Chem. Commun.* **2002**, 3016-3017.

22. (a) Luo, L.; Eisenberg, A. *J. Am. Chem. Soc.* **2001**, 123, 1012-1013. (b) Luo, L.; Eisenberg, A. *Langmuir* **2001**, 17, 6804-6811.

23. Liu, F.; Eisenberg, A. *J. Am. Chem. Soc.* **2003**, 125, 15059-15064.

24. Sadron, C. *Pure Appl. Chem.* **1962**, 4, 347-362.

25. Yu, Y.; Eisenberg, A. *J. Am. Chem. Soc.* **1997**, 119, 8383-8384.

26. Yu, Y.; Zhang, L.; Eisenberg, A. *Macromolecules* **1998**, 31(4), 1144-1154.

27. Choucair, A.; Lavigueur, C.; Eisenberg, A. *Langmuir* **2004**, 20(10), 3894-3900.

Chapter 4

PEO-*b*-PS-*b*-PAA Triblock Copolymer Vesicles

4.1 Abstract

The focus of this chapter is the preparation and characterization of PEO-*b*-PS-*b*-PAA triblock copolymer vesicles. Vesicles with either PEO or PAA outside have been successfully prepared in dioxane/water. These vesicles may serve as vehicles for potential encapsulation applications. The average size and corona chain composition of the triblock copolymer vesicles can be controlled by varying factors such as the PAA block length and pH. The polymer chains may have different arrangements in the vesicle wall, resulting in different corona chain compositions. The vesicles with PAA outside are stable in water, while the vesicles with PEO outside tend to flocculate. Nevertheless, the sediment can be redispersed under vigorous stirring.

4.2 Introduction

Lipid vesicles have been widely used as models for biological membranes and as prototype drug delivery systems.[1-3] However, the limited stability of these vesicles makes them impractical for applications that require robust devices. Instead, block copolymers with considerably longer hydrophobic blocks than those of lipids are known to yield stable vesicles. In the past decade, various synthetic block polymers have been reported to form vesicles, including AB diblock,[4-6] ABA[7-8] and ABC[9-11] triblock copolymers.

Diblock copolymer vesicles have been studied extensively. In our group, vesicles have been prepared from several diblock copolymers, including PS-*b*-PAA,[4] PS-*b*-PEO,[5] PBD-*b*-PAA[12] and PS-*b*-P4VP.[13] Various vesicles, such as small uniform vesicles,[4] large polydisperse vesicles,[5] entrapped vesicles[14] and onions,[15] have been found. The different vesicular structures and the average sizes of the vesicles can be controlled by a wide range of external factors, including the diblock copolymer composition, the initial copolymer concentration, the nature and composition of the common solvent, and the type and concentration of additives.[15-17] The increase of vesicle size is due to the fusion of smaller vesicles, while the decrease of vesicle size is a result of the fission of bigger vesicles.[16] The kinetics of fusion of PS-*b*-PAA vesicles have also been investigated.[18] In addition, the thermodynamic stabilization mechanism of the vesicles has been elucidated by Luo and Eisenberg.[19] The thermodynamic stabilization of block copolymer vesicles involves the preferential segregation of short hydrophilic chains to the inside of the vesicles and the long hydrophilic chains to the outside. The curvature of the vesicles is thus thermodynamically stabilized since the corona chain repulsion on the outside of the vesicle is bigger than that on the inside of the vesicles.

Discher *et al*[6] prepared vesicles from polyethylene oxide-*b*-polyethylethylene and characterized the vesicles by micromanipulation. The giant vesicles were proved to be almost an order of magnitude tougher than typical phospholipids. The vesicle membrane was also at least 10 time less permeable to water than common phospholipid bilayers.

In contrast to the extensive studies on diblock copolymer vesicles, only a few publications describe vesicle formation from ABA[7-8] and ABC[9-11] triblock copolymers. Schillén's group[7] reported the vesicle formation from PEO-*b*-PPO-*b*-PEO in dilute aqueous solution. Meier's group[8] prepared giant vesicles from poly(2-methyloxazoline)-*b*-poly(dimethylsiloxane)-*b*-poly(2-methyloxazoline). The Membranes of vesicles prepared from diblock copolymers and ABA-type triblock copolymers are symmetric if curvature is neglected; however, cell membranes are asymmetric, with different inside and outside faces. For instance, the two lipid layers may differ in specific lipid composition, and each protein has directional orientation in the cell membrane. Using ABC triblock copolymers, biomimetic vesicles with asymmetric membranes could be prepared. Yu and Eisenberg[9] obtained vesicles from PS_{180}-*b*-$PMMA_{67}$-*b*-PAA_{37}. These vesicles may have an inner PS wall and an outer PMMA wall due to the different hydrophobicity of PS and PMMA. Meier's group reported the preparation of vesicles with asymmetric memberanes from poly(ethylene oxide)-*b*–poly(dimethylsiloxane)-*b*–poly(2-methyloxazoline) with a hydrophobic middle block and two hydrophilic end blocks.[10] Their results support the thermodynamic stabilization mechanism of block copolymer vesicles previously proposed by Luo and Eisenberg[19]. Recently, Liu and Eisenberg[11] reported vesicles with either P4VP or PAA outside under different pH

conditions and the pH triggered inversion of vesicles from poly(acrylic acid)-*b*-polystyrene-*b*-poly(4-vinyl pyridine).

In this chapter, we describe the preparation and characterization of PEO-*b*-PS-*b*-PAA vesicles. Different factors that can be used to control the average size of the vesicles are reviewed. The effects of pH and the PAA block length on the corona chain composition of the vesicles are examined. The possible arrangements of hydrophobic PS chains in the vesicle wall and the stability of the vesicles are also discussed. Vesicles with PEO or PAA outside may serve as carriers for potential encapsulation applications.

4.3 Experimental

The same materials as described in Chapter 3 were used in this study. The vesicles were prepared in dioxane/water at a water content of 60% w/w by the same procedure used for aggregate preparation as also described in Chapter 3. In addition to the characterization methods specified in that chapter, electrophoresis was employed to examine the external corona chain compositions of the triblock copolymer vesicles prepared under different conditions. By comparing the zeta-potentials of the triblock copolymer vesicles with those of PS-*b*-PEO and PS-*b*-PAA vesicles at different pH, one can see if the corona of the tribloock copolymer vesicles is composed of PEO or PAA or both.

The electrophoretic mobility (m) of the dialyzed vesicle solutions was measured in 7.5 mM NaCl aqueous solutions at 25 °C over a pH range of 3-9, using a Rank Brothers MK II microelectrophoresis apparatus. The pH values of the vesicle solutions were adjusted by adding 7.5 mM HCl or NaOH aqueous solutions. The vesicle velocity

(u) under the applied electric field (field strength E) was obtained by measuring the time spent by the aggregates to travel a distance of 100 μm. The electrophoretic mobility was then calculated by the definition shown in equation (4-1):

$$m = u / E \qquad (4\text{-}1)$$

The zeta potential (ζ) was obtained using equation (4-2).[20] In this equation, ε is the permittivity of the suspending liquid and η is the viscosity. *f(Ka)* is a correction factor determined by the electric double layer thickness (K^{-1}) and the vesicle radius (*a*). *f(Ka)* was estimated from the calculations by O'Brien and White.[21]

$$\zeta = 3\ m\ \eta / 2\ \varepsilon f(Ka) \qquad (4\text{-}2)$$

4.4 Results and Discussion

4.4.1 Factors that Affect Vesicle Size

As described in Chapter 3, several factors have been found to affect the average size of the vesicles. The common solvent dioxane favors the formation of vesicles. By using solvent mixtures of THF/dioxane or DMF/dioxane, smaller vesicles could be prepared due to the increasing corona chain repulsion (Fig. 3.3 and Fig. 3.4). However, the presence of THF or DMF facilitates the formation of spherical micelles. The PAA block length also has an effect on the vesicle size. As the PAA block length increases, the average size of vesicles decreases due to the increasing corona chain repulsion (Fig. 3.5). The average size of the vesicles also decreases with increasing pH since more acrylic acid groups are ionized at higher pH, resulting in higher corona chain repulsion (Fig. 3.6). The average size of vesicles increases slightly from 82 ± 27 to 122 ± 44 nm as the initial

copolymer concentrations increases from 1.0% w/w to 3.0% w/w (Fig. 3.8). This is probably due to the increasing aggregation number with the increasing initial copolymer concentration.

4.4.2 Vesicle Corona Chain Composition

The corona chain composition is influenced by the corona chain repulsion. By increasing the corona chain repulsion between PAA chains, more PAA chains would stay outside the vesicles to stablilize the curvature. The corona chain repulsion can be varied by changing factors such as the PAA block length and pH. As the PAA block length or pH increases, the corona chain repulsion also increases, thus favoring the presence of PAA chains outside the vesicles; the increase in the PAA content on the outside has been proved by zeta-potential measurements.

Fig. 4.1 shows the zeta-potential curves of PS_{156}-*b*-PEO_{45}, PEO_{45}-*b*-PS_{156}-*b*-PAA_5, PEO_{45}-*b*-PS_{156}-*b*-PAA_{15} and PEO_{45}-*b*-PS_{156}-*b*-PAA_{28} and PS_{313}-*b*-PAA_{27} vesicles. By comparing the zeta-potential curves of the triblock copolymer vesicles with those of diblock copolymer vesicles, one can see qualitatively the corona chain composition of the triblock copolymer vesicles. The plot of PEO_{45}-*b*-PS_{156}-*b*-PAA_5 vesicles is similar to that of PS_{156}-*b*-PEO_{45} vesicles which have only PEO corona chains, indicating that the outside surface of the vesicles is composed of PEO chains; the plot of PEO_{45}-*b*-PS_{156}-*b*-PAA_{28} is similar to that of PS_{313}-*b*-PAA_{27} vesicles with only PAA corona chains, suggesting that the external corona consists of PAA chains; the plot of PEO_{45}-*b*-PS_{156}-*b*-PAA_{15} lies in between, revealing that both PAA and PEO chains are outside the vesicles.

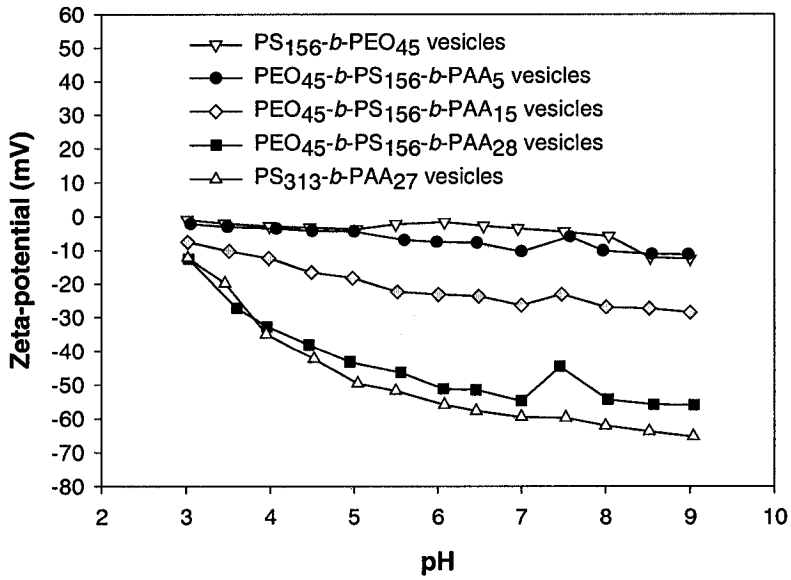

Fig. 4.1 Zeta-potential curves as a function of pH for different block copolymer vesicles.

Fig. 4.2 presents the zeta-potential curves of PEO_{45}-*b*-PS_{156}-*b*-PAA_{28} vesicles prepared at the apparent pH (pH*) 1 and 5, as well as the plots of PS_{156}-*b*-PEO_{45} and PS_{313}-*b*-PAA_{27} vesicles. The triblock copolymer vesicles prepared at pH*5 are similar to those with PAA corona chains since the zeta-potential plot of the triblock copolymer vesicles is very similar to that of the PS_{313}-*b*-PAA_{27} vesicles. The triblock copolymer vesicles prepared at pH*1 may have fewer PAA chains outside since the zeta-potential plot lies farther above that of PS_{313}-*b*-PAA_{27} vesicles. Some PEO segments may also be outside since the zeta-potential plot lies in between those of PS_{156}-*b*-PEO_{45} and PS_{313}-*b*-PAA_{27} vesicles.

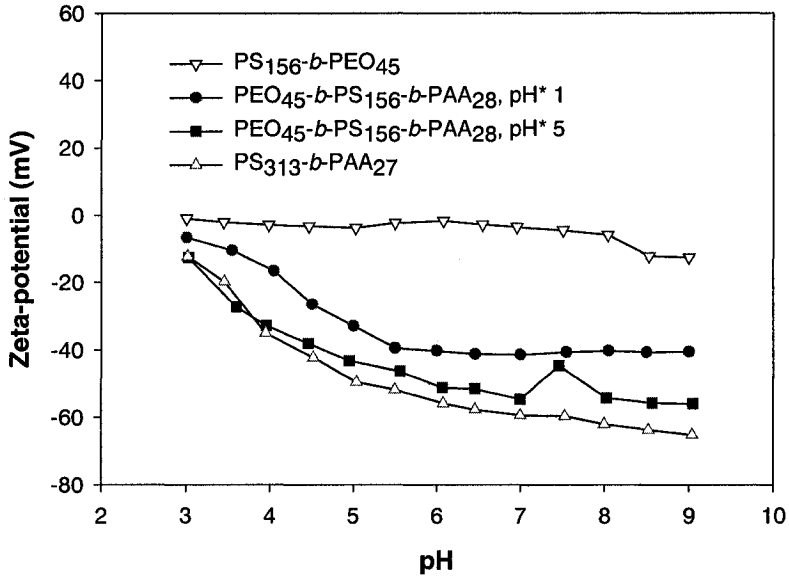

Fig. 4.2 Zeta-potential measurements for vesicles fromPS_{156}-*b*-PEO_{45}, PEO_{45}-*b*-PS_{156}-*b*-PAA_{28} and PS_{313}-*b*-PAA_{27}.

4.4.3 Proposed Arrangements of Polymer Chains in the Vesicle Wall

As described in chapter 3 (Fig. 3.5), the PEO_{45}-*b*-PS_{156}-*b*-PAA_5 vesicles have an average diameter of 433 ± 155 nm and an average wall thickness of 22 ± 3 nm; the PEO_{45}-*b*-PS_{156}-*b*-PAA_{15} vesicles have an average diameter of 336 ± 132 nm and an average wall thickness of 13 ± 2 nm; the PEO_{45}-*b*-PS_{156}-*b*-PAA_{28} vesicles have an average diameter of 82 ± 27 nm and an average wall thickness of 14 ± 2 nm. The difference in the size and wall thickness of the vesicles suggests that the polymer chains may have different arrangements in vesicle wall.

For PEO_{45}-*b*-PS_{156}-*b*-PAA_5 vesicles, the vesicle wall thickness is *ca.* 1.8 times smaller than the length of a completely stretched planar zigzag hydrophobic block of 156

PS units (*ca.* 39 nm, taking the C-C-C bond angle 109.5°) but about seven times bigger than the root-mean-square end-to-end distance of the PS block (*ca.* 3.1 nm). It is possible that the triblock copolymer behaves like a PS-*b*-PEO diblock copolymer and forms vesicles with the symmetric membrane structure as shown in Fig. 4.3. The corona chains inside and outside the vesicles consist of PEO, while the vesicle wall has a sandwich structure with the short PAA chains in the middle. The enthalpy penalty of locating the short hydrophilic PAA chains in the hydrophobic vesicle wall could be balanced by the decrease of the interfacial energy though the decrease of the total interfacial area between PS chains and water.

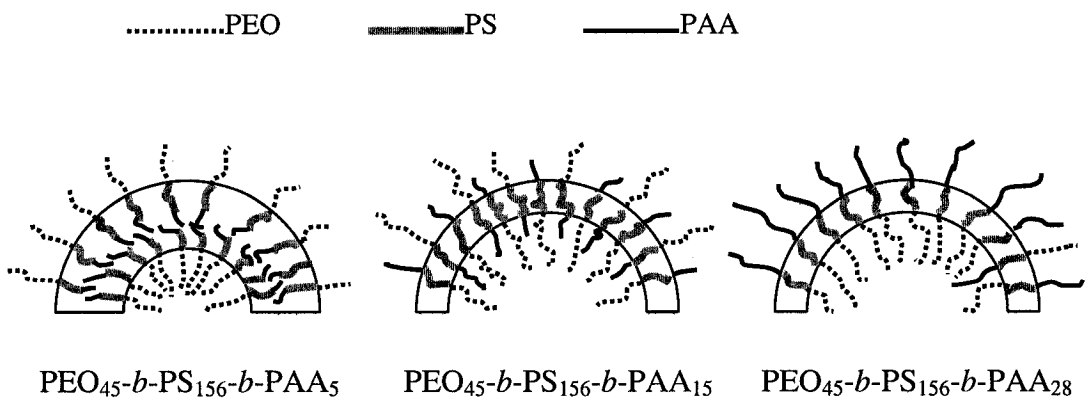

Fig. 4.3 Proposed arrangements of polymer chains in vesicle wall for vesicles prepared from PEO_{45}-*b*-PS_{156}-*b*-PAA_5, PEO_{45}-*b*-PS_{156}-*b*-PAA_{15} and PEO_{45}-*b*-PS_{156}-*b*-PAA_{28}.

For PEO_{45}-*b*-PS_{156}-*b*-PAA_{15} and PEO_{45}-*b*-PS_{156}-*b*-PAA_{28} vesicles, the vesicle wall thickness is around three times smaller than the length of the fully stretched PS block It is thus possible that a majority of polymer chains would span the vesicle wall. According to the results of zeta-potential measurements, the PEO_{45}-*b*-PS_{156}-*b*-PAA_{15}

vesicles have both PEO and PAA outside, while the PEO_{45}-*b*-PS_{156}-*b*-PAA_{28} vesicles have mostly PAA chains outside, as suggested in Fig. 4.3.

4.4.4 Stability of Vesicles in Water

The vesicles with PAA outside are stable in water, while the vesicles with PEO outside tend to floculate. Nevertheless, the sediment can be redispersed under vigorous stirring. It is well known that the stability of a colloid dispersion depends on the balance of the repulsive and attractive forces that exist between the colloid particles. If the repulsive forces are much stronger than the attractive forces, the colloid will be stable. However, if there is little or no repulsive force, then eventually flocculation or aggregation will occur. The zeta potential of a particle gives an approximate idea of the surface potential of the particle, and thus the magnitude of the measured zeta potential can be used to estimate the magnitude of the repulsive force and predict the long-term stability of a colloid dispersion. As shown in Fig. 4.4, the zeta-potential of the vesicles with PEO outside is close to zero at neutral pH, while the zeta-potential of the vesicles with PAA outside is around –60 mV, providing stability of the vesicles at neutral pH.

4.5 Conclusions

PEO-*b*-PS-*b*-PAA triblock copolymer vesicles with either PEO or PAA outside have been successfully prepared in dioxane/water. The average size and corona chain composition of the triblock copolymer vesicles can be controlled by varying factors such as the PAA block length and pH. As the PAA block length or pH increases, the average size of vesicles decreases due to increasing corona chain repulsion. The polymer chains

may have different arrangements in the vesicle wall, resulting in different corona chain compositions. The vesicles with PAA outside are stable in water, while the vesicles with PEO outside tend to flocculate. Nevertheless, the sediment can be redispersed under vigorous stirring. The stability of the vesicles in water is related to the zeta-potential values that can be used to estimate the repulsive forces between the vesicles. The zeta-potential of the vesicles with PEO outside is close to zero at neutral pH, and the steric stabilization of PEO may not be strong enough to provide long-term stability of the vesicles, while the zeta-potential of the vesicles with PAA outside is around –60 mV, providing stability of the vesicles at neutral pH.

4.6 References

1. McMaster, C. R. *Biochem. Cell. Biol.* **2001**, 79(6), 681-692.
2. Westhaus, E.; Messersmith, P. B. *Biomaterials* **2001**, 22(5), 453-462.
3. Cevc, G. *Adv. drug deliver rev.* **2004**, 56(5), 675-711.
4. Zhang, L.; Eisenberg, A. *Science* **1995**, 268, 727-731.
5. Yu, K.; Zhang, L.; Eisenberg, A. *Langmuir* **1996**, 12(25), 5980-5984.
6. Discher, B. M.; Won, Y.-Y.; Ege, D. S.; Lee, J. C.-M.; Bates, F. S.; Discher, D. E.; Hammer, D. A. *Science* **1999**, 284(5417), 1143-1146.
7. Schillén, K.; Bryskhe, K.; Mel'nikova Y. S. *Macromolecules* **1999**, 32, 6885-6888.
8. Sauer, M; Haefele, T; Graff, A; Nardin, C; Meier, W. *Chem. Commun.* **2001**, (23), 2452-2453.
9. Yu, G. E.; Eisenberg, A. *Macromolecules* **1998**, 31, 5546-5549.
10. Stoenescu, R.; Meier, W. *Chem. Commun.* **2002**, 3016-3017.

11. Liu, F.; Eisenberg, A. *J. Am. Chem. Soc.* **2003**, 125, 15059-15064.

12. Yu, Y.; Zhang, L.; Eisenberg, A. *Langmuir* **1997**, 13(9), 2578-2581.

13. Shen, H.; Zhang, L.; Eisenberg, A. *J. Am. Chem. Soc.* **1999**, 121(12), 2728-2740.

14. Yu, Y.; Zhang, L.; Eisenberg, A. *Macromolecules* **1998**, 31(4), 1144-1154.

15. Shen, H.; Eisenberg, A. *Angew. Chem. Int. Ed.* **2000**, 39(18), 3310-3312.

16. Luo, L.; Eisenberg, A. *Langmuir* **2001**, 17(22), 6804-6811.

17. Choucair, A.; Lavigueur, C.; Eisenberg, A. *Langmuir* **2004**, 20(10), 3894-3900.

18. Choucair, A.; Kycia, A. H.; Eisenberg, A. *Langmuir* **2003**, 19(4), 1001-1008.

19. Luo, L.; Eisenberg, A. *J. Am. Chem. Soc.* **2001**, 123(5), 1012-1013.

20. Shaw, D. J. *Introduction to Colloid and Surface Chemistry,* 4th ed.; Butterworth-Heinemann: Oxford, **1992**, p175-209.

21. O'Brien, R. W.; White, L. R. *J. Chem. Soc. Faraday II* **1978**, *74*, 1607-1626.

Chapter 5

Conclusions, Contributions to Original Knowledge, and Suggestions for Future Work

5.1 Conclusions and Contributions to Original Knowledge

The studies presented in this thesis explored the synthesis of the PEO-*b*-PS-*b*-PAA triblock copolymers with relatively short PEO and PAA blocks and the self-assembly behavior of a series of three triblock copolymers with different PAA block lengths under different conditions. In particular, the size and corona chain composition control of the vesicles are elucidated. The possible arrangements of the polymer chains in the vesicle wall and the stability of the vesicles are also discussed. A summary of these findings is given in the following sections.

5.1.1 Synthesis and Characterization of PEO-*b*-PS-*b*-PAA Triblock Copolymers

The PEO-*b*-PS-*b*-PAA triblock copolymers with a long hydrophobic PS block and relatively short hydrophilic PEO and PAA blocks were synthesized using ATRP technique in four major steps. First, a bromo-terminated PEO macro-initiator was prepared by the esterification of monomethoxy-capped PEO with 2-bromoisobutyryl bromide. The second step involves in the ATRP of styrene in bulk using the catalyst

system CuBr/bipyridine (bpy). The third step is the ATRP of *t*-BA in THF to obtain the PEO-*b*-PS-*b*-P*t*BA parent triblock copolymers. The catalyst system is CuBr/*N,N,N',N',N''*-pentamethyldiethylenetriamine (PMDETA). The PEO-*b*-PS-*b*-PAA triblock copolymers were prepared through the hydrolysis of the parent triblock copolymers mediated by trifluoroacetic acid.

IR and ^{1}H NMR measurements confirmed the formation of the macro-initiators and the triblock copolymers. The compositions of the copolymers were calculated from the integrals of the proton peaks in the ^{1}H NMR spectra. GPC yielded unreliable molecular weights for the PEO-containing polymers due to the difference in hydrodynamic properties of the polymers and the polystyrene standards used in the calibration, so the molecular weights were calculated according to compositions determined by ^{1}H NMR. Nevertheless, GPC is useful to determine the polydispersity indexes of the polymers. The GPC chromatographs of the macro-initiators and the parent triblock copolymer show unimodal peaks. In addition, the polydispersity indexes of all the copolymers are relatively low ($M_w/M_n < 1.3$), indicating that the polymerizations were controlled.

The effect of polymerization time on the bulk ATRP of styrene was studied. The average length of PS block and polydispersity index gradually increased with increasing polymerization time. The effect of $CuBr_2$ in the catalyst system for the ATRP of *t*-BA in THF was also investigated. The average length of P*t*BA block can be adjusted by varying the amount of $CuBr_2$ in the catalyst system. Shorter P*t*BA block was obtained by increasing the amount of $CuBr_2$. Unlike the bulk ATRP of *t*-BA,[1] no significant effect of temperature was found. The average length of P*t*BA block increased slightly from 28 to

32 as the temperature increased from 60°C to 75°C but the polydispersity remained relatively low.

5.1.2 Multiple Morphologies of PEO-*b*-PS-*b*-PAA Triblock Copolymers in Solution

Multiple morphologies have been found for the PEO-*b*-PS-*b*-PAA triblock copolymers with a long hydrophobic PS block and relatively short hydrophilic PEO and PAA blocks under various preparatory conditions. The effects of several factors on the aggregate size and morphology were investigated.

The solvent has a significant effect on the aggregate morphologies. No aggregates were found in DMF, while spheres were prepared in THF and vesicles were obtained in dioxane. This is probably because the micellization is mainly controlled by the corona chain repulsion. The degree of corona chain repulsion is related to the dielectric constants (ε) of the solvents as suggested by Yu and Eisenberg.[2] The ε values of DMF, THF and dioxane are 38.2, 7.5 and 2.2, respectively.[2] The corona chain repulsion is highest in DMF since more acrylic acid groups are ionized due to its highest dielectric constant. Although no aggregates were seen in DMF, monomolecular micelles with a compact insoluble PS core may have formed. In addition, the PEO may also provide steric stabilization of the monomolecular micelles, further preventing the formation of polymolecular aggregates. The corona chain repulsion is lower in THF than in DMF, so the single chains start to aggregate into spherical micelles. In dioxane, the corona chain repulsion is the lowest and vesicles are found.

Solvent mixtures of THF/dioxane and DMF/dioxane have also been used to study whether a progressive change in the nature of the common solvent would be accompanied by gradual changes in the aggregate morphology. As the content of THF or DMF increases, more spheres tend to form and the size of vesicles decreases. DMF has a more significant effect than THF. By adding 25% w/w DMF to the solvent mixture, only spheres were found, while both vesicles and spheres were present with the same content of THF in the solvent mixture.

The PAA block length has a significant effect on the vesicle size. This is mainly due to the varied corona chain repulsion with different PAA block lengths. With a shorter PAA block length, the corona chain repulsion is lower, resulting in the formation of bigger vesicles due to the increasing radius of curvature.[3]

The pH also influences the aggregate size and morphology. At the apparent pH (pH*) of 1, big vesicles with an average diameter of 192 $\pm$ 98 nm are observed, while at pH*5, smaller vesicles with an average diameter of 82 $\pm$ 27 nm are found. At pH*13, small lamellae and rods are seen. The decrease of the vesicle size is due to the increasing corona chain repulsion with the increasing pH.[3] The corona chain repulsion becomes bigger at higher pH since more acrylic acid groups are ionized. As the pH* changes from 5 to 13, the corona chain repulsion increases significantly, leading to the conversion of vesicles into small lamellae and rods.

The effect of water content on the vesicle size is a balance of the effects of the interfacial energy and the corona chain repulsion.[3] As the water content increases, both the interfacial energy and the corona chain repulsion increase. However, the increasing interfacial energy favors the formation of bigger vesicles, while the increasing corona

chain repulsion facilitates the formation of smaller vesicles. Since no change occurs to the average size of the vesicles, the two effects must conteract.

The initial copolymer concentration also affects the vesicle size. The average size of vesicles increases slightly from 82 $\pm$ 27 to 122 $\pm$ 44 nm as the initial copolymer concentrations increases from 1.0% w/w to 3.0% w/w. This is probably due to the increasing aggregation number with the increasing initial copolymer concentration.

5.1.3 PEO-*b*-PS-*b*-PAA Triblock Copolymer Vesicles

PEO-*b*-PS-*b*-PAA triblock copolymer vesicles with either PEO or PAA outside have been successfully prepared in dioxane/water. The average size and corona chain composition of the triblock copolymer vesicles can be controlled by varying factors such as the PAA block length and pH. As the PAA block length or pH increases, the corona chain repulsion increases, thus favoring the presence of PAA chains outside the vesicles to stabilize the curvature. The polymer chains may have different arrangements in the vesicle wall, resulting in different corona chain compositions.

The vesicles with PAA outside are stable in water, while the vesicles with PEO outside tend to flocculate. Nevertheless, the sediment can be redispersed under vigorous stirring. The stability of the vesicles in water is related to the zeta-potential values. The zeta-potential gives an approximate idea of the surface potential that can be used to estimate the repulsive forces between the vesicles. The zeta-potential of the vesicles with PEO outside is close to zero at neutral pH, and the steric stabilization of PEO may not be strong enough to provide long-term stability of the vesicles, while the zeta-potential of

the vesicles with PAA outside is around –60 mV, providing stability of the vesicles at neutral pH.

5.2 Suggestions for Future Work

5.2.1 Synthesis of PEO-*b*-PS-*b*-PAA Triblock Copolymers with Varied Block Lengths of PEO or PS

Since the block length of PAA has a significant effect on the size and corona chain composition of the triblock copolymer vesicles, one might be interested in triblock copolymer series with different block lengths of PEO or PS. It would be interesting to see if these factors could offer better control over the aggregate morphology.

5.2.2 Triblock Copolymer Vesicles with PEO or PAA Outside as Models for Loading and Release of Fluorescent Dyes

The vesicles with either PAA or PEO outside may serve as models for loading and release of fluorescent dyes. Since the surface charges of the two types of vesicles are considerably different, it would be interesting to examine if surface charge has a significant effect on the loading and subsequent release of different fluorescent dyes.

5.3 References

1. Ma, Q.; Wooley, K. L. *J. Polym. Sci. Part A: Polym. Chem.* **2000**, 38, 4805-4820.

2. Yu, Y.; Eisenberg, A. *J. Am. Chem. Soc.* **1997**, 119, 8383-8384.

3. Choucair, A.; Lavigueur, C.; Eisenberg, A. *Langmuir* **2004**, 20(10), 3894-3900.